bioRxiv preprint doi: https://doi.org/10.1101/106989; this version posted February 8, 2017. The copyright holder for this preprint (which was not certified by peer review) is the author/funder, who has granted bioRxiv a license to display the preprint in perpetuity. It is made available under aCC-BY-NC-ND 4.0 International license.

Habitat generalists or specialists, insights from comparative genomic analyses of *Thermosipho* lineages

Thomas H.A. Haverkamp[1*], Claire Geslin[2,3,4], Julien Lossouarn[2,3,4], Olga A. Podosokorskaya[5], Ilya Kublanov[5,6], Camilla L. Nesbø[1,7]

* Corresponding author

[1] Centre for Ecological and Evolutionary Synthesis, University of Oslo, Oslo, Norway

[2]Université de Bretagne Occidentale (UBO), Institut Universitaire Européen de la Mer (IUEM) – UMR 6197, Laboratoire de Microbiologie des Environnements Extrêmes (LMEE), rue Dumont d'Urville, F-29280 Plouzané, France.

[3]CNRS, IUEM – UMR 6197, Laboratoire de Microbiologie des Environnements Extrêmes (LMEE), rue Dumont d'Urville, F-29280 Plouzané, France.

[4]Ifremer, UMR 6197, Laboratoire de Microbiologie des Environnements Extrêmes (LMEE), Technopôle Pointe du diable, F-29280 Plouzané, France.

[5]Winogradsky Institute of Microbiology, Research Center of Biotechnology, Russian Academy of Sciences, Moscow, Russia.

[6]Immanuel Kant Baltic Federal University, Kaliningrad, Russia.

[7] Department of Biological Sciences, University of Alberta, Edmonton, AB, Canada

Keywords: Extremophiles, hydrothermal vents, mobile DNA, speciation, Thermotogae, Vitamine B12

bioRxiv preprint doi: https://doi.org/10.1101/106989; this version posted February 8, 2017. The copyright holder for this preprint (which was not certified by peer review) is the author/funder, who has granted bioRxiv a license to display the preprint in perpetuity. It is made available under aCC-BY-NC-ND 4.0 International license.

Abstract

Thermosipho species inhabit various extreme environments such as marine hydrothermal vents, petroleum reservoirs and terrestrial hot springs. A 16S rRNA phylogeny of available *Thermosipho* spp. sequences suggested habitat specialists adapted to living in hydrothermal vents only, and habitat generalists inhabiting oil reservoirs, hydrothermal vents and hotsprings. Comparative genomics and recombination analysis of the genomes of 15 *Thermosipho* isolates separated them into three species with different habitat distributions, the widely distributed *T. africanus* and the more specialized, *T. melanesiensis* and *T. affectus*. The three *Thermosipho* species can also be differentiated on the basis of genome content. For instance the *T. africanus* genomes had the largest repertoire of carbohydrate metabolism, which could explain why these isolates were obtained from ecologically more divergent habitats. The three species also show different capacities for defense against foreign DNA. *T. melanesiensis* and *T. africanus* both had a complete RM system, while this was missing in *T. affectus*. These observations also correlated with Pacbio sequencing, which revealed a methylated *T. melanesiensis* BI431 genome, while no methylation was detected among two *T. affectus* isolates. All the genomes carry CRISPR arrays accompanied by more or less complete CRISPR-cas systems. Interestingly, some isolates of both *T. melanesiensis* and *T. africanus* carry integrated prophage elements, with spacers matching these in their CRISPR arrays. Taken together, the comparative genomic analyses of *Thermosipho* spp. revealed genetic variation allowing habitat differentiation within the genus as well as differentiation with respect to invading mobile DNA that is present in subsurface ecosystems.

bioRxiv preprint doi: https://doi.org/10.1101/106989; this version posted February 8, 2017. The copyright holder for this preprint (which was not certified by peer review) is the author/funder, who has granted bioRxiv a license to display the preprint in perpetuity. It is made available under aCC-BY-NC-ND 4.0 International license.

Introduction

Bacteria of the genus *Thermosipho* belong to phylum Thermotogae and are found in high temperature environments such as deep-sea hydrothermal vents, and subsurface oil reservoirs (Antoine et al. 1997; Takai & Horikoshi 2000; Dahle et al. 2008). There are currently eight described *Thermosipho* species: *T. africanus*, *T. activus*, *T. affectus*, *T. atlanticus*, *T. geolei*, *T. globiformans*, *T. japonicus* and *T. melanesiensis* (Mukherjee & Sengupta 2015). These are thermophilic, organotrophic, anaerobes fermenting various sugars of different complexity (e.g. glucose, starch, cellulose, etc) and peptides. While the main fermentation products of all species are H_2 and CO_2, species-specific production of compounds such as acetate, lactate, ethanol or alanine have been described (Swithers et al. 2011).

Comparative genomic analyses of Thermotogae bacteria, including *Thermosipho*, have revealed complex evolutionary histories with extensive horizontal gene transfer (HGT), particularly involving members of the bacterial phylum Firmicutes and the Archaea domain (Enright et al. 2002). Most of the unique genes with predicted functions in different Thermotogae lineages are classified as being involved in metabolism and particularly genes involved in carbohydrate transport and degradation are numerous (Nesbø et al. 2002; Zhaxybayeva et al. 2009). In agreement with this, Thermotogae and *Thermosipho* species in particular, are commonly distinguished by being able to grow on different substrates. For instance, *T. affectus* and *T. activus* are able to degrade cellulose compounds, while others cannot (e.g. *T. africanus*) (Podosokorskaya et al. 2014). *T. japonicus* is able to degrade casein as the sole carbon source in conjunction with the electron acceptor thiosulfate ($Na_2S_2O_3$) (Takai & Horikoshi 2000). How such metabolic differences are encoded in the genomes and what pathways are involved is unresolved. Furthermore, how do the genetic differences

bioRxiv preprint doi: https://doi.org/10.1101/106989; this version posted February 8, 2017. The copyright holder for this preprint (which was not certified by peer review) is the author/funder, who has granted bioRxiv a license to display the preprint in perpetuity. It is made available under aCC-BY-NC-ND 4.0 International license.

71 correlate with the diversity found in the *Thermosipho* genus and the ecosystems that they
72 occupy?

73 One feature of the *Thermosipho* genus that has been studied at the genome level is the
74 presence of the vitamine B12 synthesis pathway in several *Thermosipho* isolates, but is absent
75 in other Thermotogae (Swithers et al. 2011). The genes needed for the vitamin B12 pathway
76 were acquired horizontally from the phylum Firmicutes. The acquisition of novel genetic
77 material in this way allows prokaryotes to establish novel metabolic capacities and develop
78 specific adaptations which may lead to species differentiation and innovation (Koonin 2015).
79 In addition, HGT is suggested to be important in the long-term maintenance and repair of
80 genomic information, by replacing inactivated genes by active ones (Takeuchi et al. 2014).
81 HGT can take place via transformation (naked DNA), conjugation (plasmids), transduction
82 (viruses), or transposition (transposable elements) but also with gene transfer agents (GTA's),
83 nanotubes or membrane vesicles produced by the microorganisms themselves (Darmon &
84 Leach 2014).

85 Although novel DNA may be beneficial to microorganisms (Darmon & Leach 2014),
86 viruses (and many mobile elements) can be without doubt harmful for cells, and prokaryotes
87 have developed defense methods. Several mechanisms exist that regulate the activity of
88 mobile DNA inside the cell (Westra et al. 2012), such as the restriction-modification (RM)
89 system, abortive infection (ABi) mechanisms, the clustered regulatory interspaced short
90 palindromic repeats (CRISPR) system and the recently described bacteriophage exclusion
91 (BREX) system (Stern & Sorek 2011; Goldfarb et al. 2015). CRISPRs seems to be
92 particularly important in thermophiles (Weinberger et al. 2012), and have been identified in
93 all Thermotogae genomes characterized to date including two *Thermosipho* genomes (Nesbø
94 et al. 2009; Zhaxybayeva et al. 2009). The CRISPR associated genes (cas-genes) are essential
95 for the adaptation step in the CRISPR defense system where spacers from invading DNA are

bioRxiv preprint doi: https://doi.org/10.1101/106989; this version posted February 8, 2017. The copyright holder for this preprint (which was not certified by peer review) is the author/funder, who has granted bioRxiv a license to display the preprint in perpetuity. It is made available under aCC-BY-NC-ND 4.0 International license.

96 acquired and inserted in the CRISPR array (Makarova et al. 2015). Interestingly, most of the
97 CRISPR associated genes (Cas) show evidence of HGT when comparing *T. africanus* to
98 *Thermotoga maritima* (Nesbø et al. 2009).

99 The well-studied bacterial RM system is almost universally found in both bacteria and
100 archaea (Roberts et al. 2010). The RM system uses methylation to distinguish between self
101 and foreign DNA, and is found in most bacterial genomes (Roberts et al. 2010; Vasu &
102 Nagaraja 2013). The system works by protecting methylated DNA from restriction enzymes.
103 Those enzymes will therefore only degrade invading mobile DNA that is not methylated.
104 Although the RM system is well studied, it is only poorly characterized among the
105 Thermotogae species described so far (Xu et al. 2011). For the genus *Thermosipho* in
106 particular, it is still unclear if RM systems are present, functional, and how it is involved in
107 the maintenance of genome stability when these populations have a high quantity of HGT
108 acquired genes.

109 In light of the high numbers of horizontally acquired genes within the Thermotogae it
110 is interesting that within the species *Thermotoga maritima* we found highly similar genomes
111 (Nesbø et al. 2015). This is remarkable when considering the isolation sources of the different
112 strains (The Azores, Italy, Japan, Kuril Islands (Russia) and the North Sea), which span the
113 earth, and suggests high levels of gene flow between distant subpopulations and active
114 mechanisms to maintain highly similar genomes (Nesbø et al. 2015).

115 Here we present a comparative analysis of 15 *Thermosipho* genomes, thirteen of
116 which are novel sequences generated in this study. The isolates included in this analysis were
117 obtained from deep-sea hydrothermal vents and produced fluids from oil reservoirs. The
118 genomes fall into three well-defined lineages (or species) with isolates from the same sample
119 sites showing very high similarities to each other. We show that the three species differ in
120 genomic content with regard to metabolic systems involved in carbohydrate and coenzyme

bioRxiv preprint doi: https://doi.org/10.1101/106989; this version posted February 8, 2017. The copyright holder for this preprint (which was not certified by peer review) is the author/funder, who has granted bioRxiv a license to display the preprint in perpetuity. It is made available under aCC-BY-NC-ND 4.0 International license.

metabolism, CRISPR-cas and the RM system. In addition, we show that several of the genomes contain prophages.

bioRxiv preprint doi: https://doi.org/10.1101/106989; this version posted February 8, 2017. The copyright holder for this preprint (which was not certified by peer review) is the author/funder, who has granted bioRxiv a license to display the preprint in perpetuity. It is made available under aCC-BY-NC-ND 4.0 International license.

Materials & Methods

DNA extraction and genome sequencing.

13 *Thermosipho* strains were cultured in a modified Ravot medium as previously described in (Lossouarn et al. 2015) and used for total DNA extraction as described in (Charbonnier et al. 1992; Geslin et al. 2003). All strains, except *T. africanus* Ob7 were submitted for genome sequencing at the Norwegian Sequencing Centre (NSC, Oslo, Norway). A 300 bp insert paired end library was prepared using the genomic DNA sample prep kit (Illumina, San Diego, CA, USA) for each DNA sample. The Library was spiked with phiX DNA. Subsequently, all strains except Ob7 were sequenced on an Illumina MiSeq generating a dataset of 250 bp paired end reads.

Strain Ob7 was sequenced at University of Alberta, Canada, using an Iontorrent (Thermo Fisher Scientific, Waltham, MA, USA) approach. DNA was enzymatically sheared using the Ion Shear Plus kit (Life Technologies, Carlsbad, CA, USA) then cloned using the Ion Plus Fragment Library kit (Life Technologies) following the manufacturer's instructions. The library was then sequenced on an Ion Torrent PGM using a 316D chip and 500 flows.

Four isolates (*Thermosipho* sp. 430, 431, 1063, 1070) were selected for long read sequencing with the goal to complete the genomes and assess methylation status of the DNA. DNA's were prepared following the Pacific Biosciences instructions and sequenced at the NSC on a Pacbio RSII (Pacific Biosciences, Menlo Park, CA, USA).

Quality control and genome assembly

Pacbio sequencing of the strains 431, 1063 and 1070 produced libraries suitable for genome assembly without the addition of Illumina paired-end reads. For all strains Pacbio read filtering and error-correction were performed using version 2.1 of the Pacbio smrtportal

bioRxiv preprint doi: https://doi.org/10.1101/106989; this version posted February 8, 2017. The copyright holder for this preprint (which was not certified by peer review) is the author/funder, who has granted bioRxiv a license to display the preprint in perpetuity. It is made available under aCC-BY-NC-ND 4.0 International license.

149 (http://www.pacb.com/devnet/). Assembly and base modification detection were performed
150 using the RS_HGAP_Assembly.2 and RS_Modification_and_Motif_analysis protocols.
151 Overlapping regions between contigs were manually detected using a combination of
152 read mapping and subsequent visualization with IGV (v. 2.3.23) (Thorvaldsdottir et al. 2013).
153 This allowed us to inspect regions with low quality mappings (due to the presence of
154 duplicated regions), and similar gene annotations on both sides of a contig gap. Preliminary
155 annotations were prepared using Glimmer at the RAST server and inspected in the CLC Bio
156 main workbench (Overbeek et al. 2013). Bam files were generated by mapping MiSeq PE
157 reads using bwa version (v. 0.7.5a) to the annotated contigs (Li & Durbin 2009) and by
158 converting sam files with Samtools (v. 0.1.19). Bam files were imported into the IGV viewer
159 together with the annotated contigs (Li et al. 2009). This approach resulted in closed
160 chromosomal sequences.
161 For strain 430, we generated a combined assembly using high quality illumina MiSeq
162 reads and a smaller set of Pacbio reads (15594 subreads) in an assembly using Spades (v.
163 3.5.0.) (Bankevich et al. 2012) with kmer size set to 127. Low coverage contigs (< 2.0) were
164 discarded. The remaining contigs were checked in IGV for miss-assemblies using mapped
165 MiSeq and Pacbio reads and if detected contigs were discarded. Finally the contigs were
166 checked for unambiguously overlapping ends as described above and if detected the contigs
167 were combined.
168 The *T. africanus* Ob7 genome was assembled using NEWBLER v. 2.6 (Margulies et
169 al. 2005). The remaining strains, were assembled using CLC assembler v.7, Spades (v. 3.5.0.)
170 and Velvet (v 1.2.10) (Zerbino & Birney 2008) (Table 1). Genome assemblies were compared
171 using REAPR (v1.0.16) and the most optimal assembly for each strain was selected for
172 genome annotation with the PGAP pipeline from NCBI (Hunt et al. 2013).
173

bioRxiv preprint doi: https://doi.org/10.1101/106989; this version posted February 8, 2017. The copyright holder for this preprint (which was not certified by peer review) is the author/funder, who has granted bioRxiv a license to display the preprint in perpetuity. It is made available under aCC-BY-NC-ND 4.0 International license.

16S rRNA Phylogeny of Thermosipho species

Full-length 16S rRNA sequences were manually extracted from the annotated *Thermosipho* genome assemblies generated in this study as well as publically available genomes. Next we searched the SILVA database version SSU r122 for *Thermosipho* spp. 16S rRNA sequences with the following setting: sequence length > 1300 bp, alignment quality > 80, pintail quality > 80 (Quast et al. 2013). Matching sequences were downloaded and added to extracted 16S rRNA sequences from the de-novo sequenced genomes. Multiple identical sequences from the same strain with different accession numbers (e.g. the four 16S rRNA sequences of *T. melanesiensis* BI429, five 16S rRNA sequences *T. africanus* TCF52B) are represented by a single sequence in the dataset.

The NCBI non-redundant database was then queried using BLASTn (blast+ v 2.2.26 (Camacho et al. 2009)) with the 16S rRNA gene dataset described above, to identify *Thermosipho* sp. like 16S rRNA sequences missed with the above methods. Additional full-length sequences were downloaded from Genbank and combined with the de-novo / SILVA 16S rRNA sequences.

The final 16S rRNA gene alignment consisted of *Thermosipho* sequences combined with outgroup sequences from other Thermotogales species. The resulting alignment was used to build phylogenies using Maximum Likelihood as implemented in MEGA 6.0 (Tamura et al. 2013). and the General Time Reversible (GTR) model (G+I, 4 categories) as suggested by JModelTest v. 2.1.7 (Darriba et al. 2012).

Pangenome analysis

Blast Ring genome plots were generated using BRIG version 0.95 (Alikhan et al. 2011) running Blast+ version 2.2.28 (Camacho et al. 2009) with the following set up. The nucleotide sequence of one of the 15 *Thermosipho* genomes was used to create the blast-

bioRxiv preprint doi: https://doi.org/10.1101/106989; this version posted February 8, 2017. The copyright holder for this preprint (which was not certified by peer review) is the author/funder, who has granted bioRxiv a license to display the preprint in perpetuity. It is made available under aCC-BY-NC-ND 4.0 International license.

database with default settings. Nucleotide sequences of all coding genes were extracted from each genome (NCBI Genbank annotation) using CLC Main workbench Version 6.8.3 and were used for BLASTn analysis in BRIG with the following settings: max_target_seqs: 1; max e-value cut-off: 1.0^{-4}. Alignments with a minimum of 70% similarity were visualized with BRIG. The same procedure was used for all genomes.

Complete chromosome sequences or contigs were uploaded for all 15 genomes to the Panseq 2.0 server (https://lfz.corefacility.ca/panseq/) for pangenome analysis (Laing et al. 2010). Sequence similarity cut-off (SC) was set at 70 % to identify core-genome segments and SNP's. We used the standard settings with Panseq except: percent sequence identity cut-off set to 70%, core genome threshold: 15, BLAST word size: 11. The final alignment of the single nucleotide polymorphisms (SNPs) was loaded into splitstree and visualized as an unrooted phylogeny using the neighbor network algorithm (Huson & Bryant 2006)

Ten genome sequences (none-closed genomes of the *T. melanesiensis* cluster were excluded, due to high sequence similarity) were aligned with progressiveMauve (Mauve (v. 2.3.1) (Darling *et al.*, 2010)) using *T. africanus* H17ap60344 set as the reference and automatically calculated seed weights and minimum Locally Colinear Blocks (LCB) scores. Gaps were removed and the edited LCBs were concatenated in Geneious 8 (www.geneious.com). Recombination analysis of the concatenated alignment was done in LikeWind (Archibald & Roger 2002a; 2002b) using the maximum likelihood tree calculated in PAUP* version 4.0b10 (Swofford 2002) under a GTR+Γ+I model as the reference tree.

Pairwise tetranucleotide frequency correlation coefficients (TETRA) and Average Nucleotide identity (ANI) were calculated using the JspeciesWS webtool (http://jspecies.ribohost.com/jspeciesws/) (Richter & Rosselló-Mora 2009; Goris et al. 2007). The pair-wise TETRA values were visualized with R (version 3.2.1) using the heatmap.2

bioRxiv preprint doi: https://doi.org/10.1101/106989; this version posted February 8, 2017. The copyright holder for this preprint (which was not certified by peer review) is the author/funder, who has granted bioRxiv a license to display the preprint in perpetuity. It is made available under aCC-BY-NC-ND 4.0 International license.

function (Package gplots) and the *Thermosipho* genomes were clustered using Jaccard distances based on pairwise TETRA values (Package Vegan. version 2.3-0).

The IMG/ER Pairwise ANI calculation was used to determine the number of shared genes between each genome separately (Markowitz et al. 2009). The method uses pairwise bidirectional best nSimScan hits where similar genes share a minimum of 70% sequence identity with 70% coverage of the smaller gene. For each genome we calculated the fraction of shared genes with all other genomes. Unique genes per genome were determined using the IMG Phylogenetic profiler tool for single genes, where each genome was analyzed for the presence of genes without any homologs in all other 14 genomes. The settings were: minimum e-value of 1.0^{-5}; min percent identity: 70%; pseudogenes were excluded; the algorithm was present/absent homologs. The same tool was used to identify the presence of homologs shared with all genomes, and with only the genomes from the same cluster.

Functional comparison of genome

The 15 genomes were compared using the Clusters of Orthologous Genes (COGs) annotations. A COG reference database (version 10) was downloaded from the STRING database (http://string-db.org/). For each genome all protein sequences were aligned using BlastP, with the settings: 1 target sequence; maximum e-value: $1.0e^{-20}$; database size 1.0^{7}; tabular output. Only hits to COG database sequences were retained when the alignment was >= 70% of the length of the longest protein sequence and were used to build a protein COG classification table. The COG IDs were summarized by classifying them to any of the available COG categories (ftp://ftp.ncbi.nih.gov/pub/wolf/COGs/COG0303/cogs.csv). For the COG analysis of the species-specific genes, we used the results from the IMG phylogenetic profiler tool to identify cluster specific genes. The COG classification table was screened for cluster specific genes and summarized into COG categories.

bioRxiv preprint doi: https://doi.org/10.1101/106989; this version posted February 8, 2017. The copyright holder for this preprint (which was not certified by peer review) is the author/funder, who has granted bioRxiv a license to display the preprint in perpetuity. It is made available under aCC-BY-NC-ND 4.0 International license.

In order to statistically compare species differences of COG categories we normalized counts by total COG gene annotations, giving relative abundances per genome. R (version 3.3.0) was used to identify COG categories that were significantly different between the three species using the non-parametric Kruskal-Wallis test (p-value <= 0.01). The R-package ggplot2 (version 2.1.0) was used to generate the comparisons graphically.

Horizontal gene transfer detection

Genes putatively acquired by HGT were identified using HGTector (Zhu et al. 2014) with BLASTp (blast+ v 2.2.26). The databaser.py script was used on 6 December 2015 to download per species one representative proteome of all microorganisms from the NCBI refseq database. We compared the predicted *Thermosipho* spp. protein sequences to the reference database using the following BLAST cut-offs: E-value: 1.0^{-5}, Percentage identity: 70%, percentage coverage: 50%, and a maximum of 100 hits were returned. To determine which genes were putatively acquired by any of the strains we set the HGTector self group to the genus *Thermosipho* (NCBI taxonomy ID: 2420) and the close group to either the family Fervidobacteriaceae (NCBI taxonomy ID: 1643950), or the order Thermotogales (NCBI taxonomy ID: 2419). HGTector then analyzes the blast output from each protein for hits matching taxa belonging to either the self or close groups, or more distantly related taxa, which is used to determine which genes have likely been acquired from taxa more distantly related than the close group. When the close group was set to Fervidobacteriaceae, we identified putative HGT genes specific for *Thermosipo* sp. but not found in Fervidobacteriaceae species. This setting however, did not indicate putative HGT genes derived from other families within the Thermotogales order or beyond.

Defense genes

bioRxiv preprint doi: https://doi.org/10.1101/106989; this version posted February 8, 2017. The copyright holder for this preprint (which was not certified by peer review) is the author/funder, who has granted bioRxiv a license to display the preprint in perpetuity. It is made available under aCC-BY-NC-ND 4.0 International license.

Using the defense genes list created by Makarova et al., (2011), we screened the IMG genome Clusters of Orthologous Genes (COG) annotations for the presence of any COGs involved in any of the mobile DNA defences (Makarova et al. 2011). We summarized the identified COGs and distinguished between CRISPR-cas associated or restriction-modification (RM) system genes.

Crispr-spacer analysis.

All genomes were uploaded to CRISPR finder (http://crispr.i2bc.paris-saclay.fr/) to detect CRISPR-arrays (Grissa et al. 2007). CRISPR spacer sequences from each genome were compared using BLASTn against all *Thermosipho* sp. spacer sequences using the following settings: e-value cut-off: 1.0^{-5}, database size: 1.0^{7}, dust: no. The tabular blast results were visualized with R-statistics using the Markov Cluster Algorithm (MCL) (v1.0) and Igraph (v1.0.1) packages. Igraph was used for matrix construction. MCL was run using the matrix with the inflation set to 1.4 and max iterations set to 100 (Enright et al. 2002).

In order to search for matching sequences within the genome but outside the CRISPR arrays, e.g target genes, we masked all CRISPR arrays using maskfeat (EMBOSS v. 6.5.7 (Rice et al. 2000)). Next we ran BLASTn (v2.2.26+) using the spacers of each genome against the own genome using the following settings: e-value cut-off: 1.0^{-5}, database size: 1.0^{7}, dust: no. CRISPR array spacers were also compared against the NCBI nucleotide database to find other species with similar sequences. BLASTn was run with the settings: e-value cut-off: 1.0^{-5}, dust: no. Each genome was screened for the presence of prophages (Supplementary information for details).

Vitamine B_{12} pathway analysis

bioRxiv preprint doi: https://doi.org/10.1101/106989; this version posted February 8, 2017. The copyright holder for this preprint (which was not certified by peer review) is the author/funder, who has granted bioRxiv a license to display the preprint in perpetuity. It is made available under aCC-BY-NC-ND 4.0 International license.

297 The genes involved in the Vitamine B_{12} metabolism are found in four different gene
298 clusters (BtuFCD, Corriniod, Cobalamin, and SucCoA) in *Thermosipho* and can be regulated
299 by B_{12} riboswitches (Swithers et al. 2011). All 15 genomes were screened for the presence of
300 Cobalamin specific riboswitches using Riboswitch scanner (Mukherjee & Sengupta 2015).
301 This information was used to confirm the presence of the four gene clusters in each genome.
302 Next, we extracted the protein sequences from the *T. melanesiensis* BI429 genome involved
303 in B_{12} metabolism (Swithers et al. 2011) and used them to identify homologous genes in all
304 *Thermosipho* genomes using tBLASTn with a maximum e-value 1.0^{-20}.
305
306 *Data desposition*
307 All genomes were deposited in the Genbank database and their accession numbers are
308 found in Table 1. In addition all genomes were deposited in the IMG databases and are linked
309 to the NCBI accession numbers. The 16S rRNA alignment is available upon request from the
310 corresponding author.
311

bioRxiv preprint doi: https://doi.org/10.1101/106989; this version posted February 8, 2017. The copyright holder for this preprint (which was not certified by peer review) is the author/funder, who has granted bioRxiv a license to display the preprint in perpetuity. It is made available under aCC-BY-NC-ND 4.0 International license.

312 **Results**.

313 *Global isolation of the genus Thermosipho from hydrothermal vents and oilfields.*

314 We screened the NCBI-non-redundant (nr) database using BLASTn with *Thermosipho*
315 16S rRNA genes as probes to assess how our genomic analyses span the available
316 environmental diversity of *Thermosipho* lineages. This analysis revealed that most lineages or
317 species, e.g. *T. melanesiensis*, *T. affectus* and *T. africanus*, are well covered by our genomic
318 analysis (Figure 1, Supplementary materials Figure S1). Nonetheless, there are several
319 lineages, including *T. geolei*, *T. ferriphilus* and *T. activus*, for which we do not have genomic
320 data yet.

321 Moreover, the 16S rRNA gene phylogeny suggests ecological differences between the
322 different lineages (Figure 1). *T. africanus* isolates appear to be habitat 'generalists' and have
323 been isolated and detected in oil reservoirs, marine hydrothermal vents and terrestrial hot
324 springs. In contrast the *T. melanesiensis* and *T. affectus* lineages appear to be more specialized
325 and have only been obtained from marine hydrothermal vents. Thus one interesting question
326 is if and how these different life styles are reflected in their genomes with regard to diversity
327 and genome content.

328

329 *Genome overview*

330 The current study added 13 new genomes, with different levels of completion, to the
331 two existing ones (Table 1). All genomes share a low GC content (29.9 % - 32.7 %).
332 Interestingly, the *T. affectus* genomes are the smallest in this dataset (≈ 1.77Mbp), while the
333 T. *melanesiensis* (≈ 1.9Mbp) and *T. africanus* (≈ 2.0Mbp) genomes are larger.

334

335 *Phylogenomic analysis*

bioRxiv preprint doi: https://doi.org/10.1101/106989; this version posted February 8, 2017. The copyright holder for this preprint (which was not certified by peer review) is the author/funder, who has granted bioRxiv a license to display the preprint in perpetuity. It is made available under aCC-BY-NC-ND 4.0 International license.

Tetranucleotide frequencies can be used to calculate the genomic similarity between bacterial isolates, where pairwise similarity is expressed as tetranucleotide frequency correlation coefficients (TETRA) (Richter & Rosselló-Mora 2009). The heatmap of the TETRA values of the *Thermosipho* genomes indicated the presence of 3 groups with high intra relatedness (TETRA > 0.99) (Figure 2). Interestingly, the *T. africanus* isolates show more divergent genomes compared to the other two clusters. We obtained similar clustering results when we calculated the pairwise Average Nucleotide Identities (ANI) between the isolates (data not shown), with intracluster identities > 95% and intercluster identities < 90%. The core- and pangenome of the genus *Thermosipho* was estimated to be 1.4Mbp and 5.6Mbp, respectively (Panseq2 sequence identity cut-off (IC): 70%). Splitstree networks (Huson & Bryant 2006) using different SC showed very little differences regardless of which IC was used (data non shown). The unrooted neighbor network calculated from 427,560 core SNPs is shown in Figure 3A. The network shows three branches for the three lineages with few differences within each lineage, similar to the pattern shown in the 16S rRNA tree and the TETRA heatmap.

Finally, we used the progressive Mauve aligner to extract Locally collinear blocks (LCBs) from 10 representative *Thermosipho* genomes to build a concatenated alignment. The phylogeny based on this alignment (Supplementary materials Figure S2A) showed a similar pattern as when using single nucleotide polymorphisms (SNPs) (Figure 3A). The concatenated Mauve alignment was used for recombination detection analysis using LikeWind (Archibald & Roger 2002b), which detected numerous recombination events within each cluster. However, no recombination events were detected between the clusters suggesting that the lineages do indeed correspond to three distinct species (Supplementary materials Figure S2).

bioRxiv preprint doi: https://doi.org/10.1101/106989; this version posted February 8, 2017. The copyright holder for this preprint (which was not certified by peer review) is the author/funder, who has granted bioRxiv a license to display the preprint in perpetuity. It is made available under aCC-BY-NC-ND 4.0 International license.

Core / Pan genes

Using the IMG Pairwise ANI tool we obtained for each genome the number of genes shared with all other genomes (Figure 3B). This gave a similar pattern as obtain using TETRA, ANIb/m, with the presence of three clusters. Between the three clusters we found that less than 80 % of the genes are shared between the species (IC: 70%). These results suggest the presence of strain and species-specific genes in each of the *Thermosipho* isolates analyzed. A visual inspection of genome content using BRIG showed a similar pattern (Supplementary information; Supplementary materials Figure S3 (Alikhan et al. 2011). The genomes from the *T. melanesiensis* cluster are highly similar, with *T. melanesiensis* BI429 being the most divergent (strain-specific genes, n=33) and the others strain with just a few (BI431, n = 4) or no strain-specific genes (Table 2, Table 3, Supplementary Materials Table S1). The remaining *Thermosipho* spp. genomes have few (BI1063, n = 11) to many unique genes (H17ap60334, n=169) (Supplementary Materials Table S1).

Identification of species-specific genes indicated that each species-level lineage has a common set of genes not detected in the other strain clusters (Table 2). Using 70% IC, the *T. melanesiensis* strains have 424 (+/- 1.2) specific genes (23.0 % of total), while the *T. affectus* and *T. africanus* have 350 (+/- 2)(20.2%) and 650 (+/- 11)(33.4%) cluster specific genes respectively (Table 2). Many of the species-specific genes are hypothetical proteins (26 to 45 %). The *T. africanus* genomes have a larger proportion of species-specific genes in their genome compared to the other two species. Interestingly, when using a less stringent cut-off of 30%, the number of species-specific genes is substantially reduced, e.g. species-specific genes in *T. melanesiensis* BI429 fall to 67 genes (3%), and the proportion of strain specific genes decreases as well. Also here the *T. africanus* genomes have the most species-specific genes, while *T. affectus* isolates have the least (average 5,8 vs 3.0% of total genes per genome). This indicates that most of the species-specific genes have distantly related

bioRxiv preprint doi: https://doi.org/10.1101/106989; this version posted February 8, 2017. The copyright holder for this preprint (which was not certified by peer review) is the author/funder, who has granted bioRxiv a license to display the preprint in perpetuity. It is made available under aCC-BY-NC-ND 4.0 International license.

386 homologs in the other two species, possibly due to either sequence diversification, or
387 replacement by more distantly related homologs acquired by HGT.
388
389 *Horizontal gene transfer*
390 Interestingly, in several of the genomes of the *T. africanus* and *T. affectus* isolates we
391 detected blocks of co-localized variable genes (min - max cluster size: 4 - 31) unique for that
392 genome (Table 3). No such blocks were found between the highly similar *T. melanesiensis*
393 strains. Several of the larger blocks of strain specific genes encode integrated prophages (*T.*
394 *affectus* BI1074, *T. africanus* H17ap60334) as they could be detected by at least one prophage
395 finding tools (Supplementary information, Supplementary materials Table S1). In addition,
396 when only one of the *T. melanesiensis* genomes was used to find unique genes, we detected
397 one large block consisting of a prophage as well. This prophage was present in all *T.*
398 *melanesiensis* isolates (Haverkamp et al., manuscript in preparation). The remaining clusters
399 encode genes encoding CRISPR-cas proteins (Table 3) and genes involved in various types of
400 cellular activities. Only a few clusters are dominated by hypothetical proteins (Supplementary
401 materials Table S1).
402 The co-localization of unique genes suggests acquisition by HGT for these clusters.
403 HGTector (Zhu et al. 2014) analysis suggested that between 4.0 % (*T. affectus* BI1063) and
404 5.8 % (*T. africanus* H17ap60344) of the genes in each genome have been acquired from
405 species not belonging to the Thermotogales by HGT (Table 2, Supplementary materials Table
406 S2). The majority of the putative HGT genes (average ≈ 85%) showed similarity to genes
407 found in other orders within the Thermotogae, such as the Kosmotogales and the Petrotogales.
408 The remaining genes (average ≈ 15%) were mainly shared between the *Thermosipho* genomes
409 and genomes of Firmicutes and Euryarchaeota (Supplementary materials Table S2). Within
410 each genome about 50 % of the putative HGT genes belonged to the COG categories:

bioRxiv preprint doi: https://doi.org/10.1101/106989; this version posted February 8, 2017. The copyright holder for this preprint (which was not certified by peer review) is the author/funder, who has granted bioRxiv a license to display the preprint in perpetuity. It is made available under aCC-BY-NC-ND 4.0 International license.

411 "Carbohydrate transport and metabolism", "Energy production and conversion", or were not
412 assigned to a COG category (e.g. Hypothetical genes) (data not shown). The ratio between
413 these three categories was different for the three species, with *T. africanus* having more
414 carbohydrate genes, while *T. affectus* species had more unassigned genes. Interestingly, many
415 of the putative HGT genes could be identified in several *Thermosipho* genomes, which
416 indicates that the common ancestor of the *Thermosipho* isolates acquired most of the putative
417 HGT genes. Only a few putative HGT genes fall into the genome or species-specific gene
418 sets. This is due to the fact that most of these proteins have no high quality blastP match in
419 the genomes in the HGTector database and will therefore not classify as putative HGT.
420
421 *Genome-wide comparisons of COG categories*
422 In order to detect functional differences between the three species we compared their
423 genomic content using Clusters of Orthologous Genes (COGs) annotations (Figure 4). This
424 revealed *T. africanus* to have genomes with the highest absolute gene abundances for many
425 COG categories, which is due to the *T. africanus* genomes being larger. However, this effect
426 disappears for most categories when using relative abundances of all COGs (Figure 4A;
427 Supplementary Materials Table S3). The categories H, J, L, R and G had the largest relative
428 abundance differences between the three species ($p \leq 0.01$ for H, J and R and $p \leq 0.05$ for G
429 and L). Several other categories (B, C, I, O) had highly significant relative abundances
430 differences ($p \leq 0.01$), but absolute values were either very low (B), and relative abundance
431 differences were not very large between the species, and within species they were very similar
432 (Supplementary Materials Table S3).
433 The largest COG category is made up of Category R (General function prediction
434 only), with the *T. affectus* genomes having most genes (Figure 4). Category R is also the
435 largest group among the species-specific genes (Figure 4B). These results are in line with the

bioRxiv preprint doi: https://doi.org/10.1101/106989; this version posted February 8, 2017. The copyright holder for this preprint (which was not certified by peer review) is the author/funder, who has granted bioRxiv a license to display the preprint in perpetuity. It is made available under aCC-BY-NC-ND 4.0 International license.

436 observation that on average 42.1 %, 49.3 % and 54.8 % (*T. africanus*, *T. affectus* and *T.*
437 *melanesiensis*) of the species-specific genes lack COG annotations and are hypothetical
438 genes. Interestingly, the *T. africanus* genomes have more genes with COG categories
439 annotations, but they do show more genes with the COG category R. This difference could be
440 caused by the careful manual curation of the TCF52B genome (Nesbø et al. 2009).
441 The *T. affectus* genomes show a significantly ($p \leq 0.01$) lower relative abundance of
442 genes in category H (Coenzyme transport and metabolism category) (Figure 4A). Closer
443 inspection shows that the *T. affectus* genomes are lacking most of the genes (20 out of 22
444 genes) needed for corrinoid synthesis, except *CobT* and an ATP-binding protein (indicated as
445 ORF). A complete set of corrinoid synthesis genes are found in the genomes of *T. africanus*
446 and *T. melanesiensis*, and are essential for *de novo* vitamine B_{12} synthesis (Swithers et al.
447 2011) (Supplementary materials Figure S4). Interestingly, the cobalamide salvage pathway
448 gene cluster, which is needed for retrieving incomplete corrinoid molecules from the
449 environment, is present in the *T. affectus* genomes. This gene cluster is, however, missing its
450 *CobT*' gene. This suggests that the orphan *CobT* gene, presumably a remnant from the
451 missing corrinoid cluster, is now functioning in the cobalamide salvage pathway
452 (Supplementary materials Figure S4).
453 Large differences among the genomes were also seen for COG category G
454 (Carbohydrate transport and metabolism). In agreement with this, phenotypic differences in
455 carbohydrate metabolism is one of the main other features, to distinguish between the three
456 species (Podosokorskaya et al. 2011). Also for this category, we find that the *T. africanus*
457 genomes have relatively more genes than the other two species (Figure 4A). This difference is
458 even more pronounced for species-specific genes (Figure 4B), where *T. africanus* genomes
459 have more genes present in this category (Supplementary Materials Table S3). A screening of
460 the genomes using PFAM annotations and the carbohydrate database dbCAN (Yin et al.

bioRxiv preprint doi: https://doi.org/10.1101/106989; this version posted February 8, 2017. The copyright holder for this preprint (which was not certified by peer review) is the author/funder, who has granted bioRxiv a license to display the preprint in perpetuity. It is made available under aCC-BY-NC-ND 4.0 International license.

2012), showed a similar pattern as with the COG annotations (Supplementary information; Supplementary materials Table S4). The *T. affectus, T. melanesiensis and T. africanus* genomes contain on average: 16-17, 20 and 21-26 genes respectively that are involved in breakdown of carbohydrates (Supplementary materials Table S4). Moreover, the families, containing enzymes involved in breakdown of various beta-linked oligo- and polysaccharides (eg. cellulose, xylan, laminarin, lichenan, mannans and chitin) were found exclusively among the representatives of *T. africanus*. This shows, in line with the COG analysis, that the *T. africanus* species might be more versatile with regard to carbohydrate uptake and metabolism.

When we compared the COG categories for the species-specific genes we found even larger differences for many categories (Figure 4B). Since the *T. africanus* genomes have almost twice as many species-specific genes compared to the other two species, they also have proportionally more species-specific genes in most categories. For instance, for COG category L (Replication, recombination and repair) we find large variation in the number of genes among the three *T. africanus* strains, with TCF52B having relatively more of these genes compared to the other genomes (8.7 % vs 5.7%). Examination of the genes assigned to this category revealed that this difference is mainly due to the presence of 18 copies of transposases in the TCF52B genome.

Defense genes.

Above we identified several interesting features of the *Thermosipho* genomes, where some of the genomes have a large set of unique genes, contain large mobile elements, or have many putative HGT genes. This suggests that the defense mechanisms against mobile DNA might differ among the isolates. We therefore screened the annotated genomes for the presence of COGs that are related to defense mechanisms (Makarova et al. 2011), resulting in

bioRxiv preprint doi: https://doi.org/10.1101/106989; this version posted February 8, 2017. The copyright holder for this preprint (which was not certified by peer review) is the author/funder, who has granted bioRxiv a license to display the preprint in perpetuity. It is made available under aCC-BY-NC-ND 4.0 International license.

a list of 44 COGs that could be classified into three clusters, restriction-modification (RM) systems genes (12), CRISPR-cas genes (18) and other COG annotations (14) (Figure 5).

Overall, the *T. affectus* genomes and *T. africanus* TCF52B have the most CRISPR-cas genes (Figure 5). Specifically, we observed that all the *Thermosipho* genomes contain *cas10* /*crm2* (COG1353), which indicates the usage of the type III CRISPR-cas system (Supplementary materials Table S5) (Makarova et al. 2015). The *cas10*/*crm2 (*COG1353) annotated genes are present at multiple loci in *T. affectus* and *T. melanesiensis* strains, but only one copy is found in *T. africanus* isolates. For the proper functioning of the type III system, *crm6* (COG1604) is needed. However, this gene is missing in *T. africanus* H17ap60334, suggesting an incomplete and possibly non-functioning CRISPR-cas system (Makarova et al. 2015). Furthermore, the *T. africanus* H17ap60334 genome has a lower number of CRISPR-cas genes compared to the other isolates (Figure 5; Supplementary materials Table S5). All the *T. melanesiensis* strains (except BI431) and *T. africanus* strain TCF52B also carry the type I CRISPR-cas system (marker gene: *cas3* (COG1203)). This gene is not detected in the *T. affectus* or *T. africanus* Ob7 and H17ap60334 genomes, suggesting there are differences in the mechanism of the CRISPR-cas system both within and between the *Thermosipho* isolates / species.

We also detect differences in RM systems-gene content. The *T. affectus* genomes contain few RM system genes and the *T. melanesiensis* have the most (Figure 5; Supplementary materials Table S5). For a functioning RM system both the methylase and restriction enzymes are needed. The restriction enzymes are absent from the *T. affectus* genomes, which suggest that this species does not possess a functional RM-system (Supplementary materials Table S4). In contrast, we detected both type I, II and III restriction enzymes and DNA methylases in the *T. melanesiensis* genomes. In the *T. africanus* isolates a complete type II system is present in the genomes of strains Ob7 and H17ap60334. In

bioRxiv preprint doi: https://doi.org/10.1101/106989; this version posted February 8, 2017. The copyright holder for this preprint (which was not certified by peer review) is the author/funder, who has granted bioRxiv a license to display the preprint in perpetuity. It is made available under aCC-BY-NC-ND 4.0 International license.

addition, all the *T. africanus* strains have a complete type III RM system (Supplementary materials Table S5).

In agreement with the distribution of RM-systems, Pacbio sequencing of *T. melanesiensis* BI431 and *T. affectus* BI1063 and BI1070 revealed that strain BI431 was methylated, while the two *T. affectus* genomes lacked methylation. The *T. melanesiensis* BI431 methylation sites detected matched those predicted in the Rebase restriction database (Roberts et al. 2015); both methyl-6-adenosine (m6A) and methyl-4-cytosine (m4C) methylation were detected along the entire BI431 genome. The dominant methylation sites indicate that methylation was mainly due to the type II and III systems (Table 4). We did not perform Pacbio sequencing of the *T. africanus* genomes, but the presence of a type-III methylase enzyme suitable for a functional RM-system suggests the possibility of a methylated genome.

CRISPR array variation

Between four and six CRISPR arrays were detected in all the genomes, except for *T. africanus* TCF52B, which contains 12 arrays (Table 2, Table 5, supplementary materials table S6). The total number of spacers detected in all genomes was 1709, with spacer count varying between 54 (*T. affectus* BI1223) to 321(*T. africanus* TCF52B). All the spacers could be clustered into 1001 different clusters, indicating that there are both shared and unique spacers. For instance, the highly similar *T. melanesiensis* genomes all have 5 CRISPR arrays, with a total of 681 spacers that form 92 clusters that are present in all *T. melanesiensis* genomes (Supplementary material Figure S5A). The only difference observed between these genomes was strain BI429 missing four spacers found in the other genomes. Interestingly, six of the 92 clusters have spacers from different arrays (Supplementary material Figure S5A).

bioRxiv preprint doi: https://doi.org/10.1101/106989; this version posted February 8, 2017. The copyright holder for this preprint (which was not certified by peer review) is the author/funder, who has granted bioRxiv a license to display the preprint in perpetuity. It is made available under aCC-BY-NC-ND 4.0 International license.

534 The other two species show much more diversity in comparison to *T. melanesiensis*,
535 within the spacer sequence content between the strains of the different species
536 (Supplementary material Figure S5 B and C). The *T. affectus* spp. CRISPR array spacers
537 (n=412) fall into 366 clusters, while the *T. africanus* spp. CRISPR array spacers (n= 616)
538 form 543 clusters.
539 Comparing spacer sequences to the host genome (excluding CRISPR arrays, blastN e-
540 value cut-off: 1.0^{-5}) revealed a small fraction of the spacers with matches within its host
541 genome (percentage identity 88-100%) (Table 5). The *T. affectus* genome spacers did not
542 match with any region in the host genome. For the *T. melanesiensis* genomes one spacer
543 (array 2, spacer 5) matched one gene (e.g. *T. melanesiensis* BI429: Tmel_1466: hypothetical
544 protein) in all genomes (81.8% identity, 6 SNPs). This gene is located within a prophage
545 element consisting of 50 protein coding genes (Tmel_1439 : Tmel_1486) (Haverkamp et al.,
546 in prep). The relatively low similarity between the spacer and the gene sequence could
547 suggests that this gene is not or no longer a target sequence, but we can not exclude it (Cady
548 & O'Toole 2011).
549 For the *T. africanus* genomes we detected one CRISPR spacer, shared by all three
550 genomes, which has a non-perfect match to the same genomic region. The spacer matches a
551 phospholipase / carboxylesterase gene (THA_1282 in strain TCF52B) with 89-92% identity.
552 For *T. africanus* H17ap60334 we find three additional spacers with perfect matches in two of
553 its gene; two spacers target H17ap60334_04822 and one targets H17ap60334_04912. Closer
554 examination revealed that also these genes are part of a predicted prophage region
555 (Haverkamp et al., in prep.; Supplementary information).
556 Finally, we searched NCBI's non-redundant nucleotide database for matches to the
557 *Thermosipho* spacer sequences. This identified two identical 44 bp spacers, one in *T.*
558 *africanus* H17ap60334 (array 2, spacer 7) and one in *T. africanus* TCF52B (array 5, spacer

bioRxiv preprint doi: https://doi.org/10.1101/106989; this version posted February 8, 2017. The copyright holder for this preprint (which was not certified by peer review) is the author/funder, who has granted bioRxiv a license to display the preprint in perpetuity. It is made available under aCC-BY-NC-ND 4.0 International license.

559 20) that matched a sequence in the genome of *Pseudothermotoga elfii* DSM 9442 (genbank
560 refseq ID: NC_022792). The identified region in that genome (bp 200095 – 200125) is a
561 CRISPR spacer sequence of 38bp, which is identical to the *Thermosipho* spacer for 31 bases.
562 Interestingly, the first six bases of the *Pseudothermotoga* spacer has no match to the
563 *Thermosipho* H17ap60334 and TCF52B spacer, while the last 12 bases of the *Thermosipho*
564 spacers have no match to the *Pseudothermotoga* spacer. This suggests the spacers in both
565 species were acquired independently, but that they match a similar sequence.
566

bioRxiv preprint doi: https://doi.org/10.1101/106989; this version posted February 8, 2017. The copyright holder for this preprint (which was not certified by peer review) is the author/funder, who has granted bioRxiv a license to display the preprint in perpetuity. It is made available under aCC-BY-NC-ND 4.0 International license.

Discussion

Bacterial genome stability and evolution are under influence of HGT, which, among other things, may influence how quickly a new species will arise (Darmon & Leach 2014). For instance, low levels of DNA exchange, within species, will allow mutations to arise quicker than homologous recombination can repair it leading to speciation events, while high levels of within species DNA exchange, prevents strains from accumulating enough mutations to differentiate (Lawrence & Retchless 2009). High levels of HGT have previously been observed for Thermotogae bacteria, in particular the *Thermotoga* genus, which is found in high temperature ecosystems, comparable to those where *Thermosipho* occurs (Nelson et al. 1999; Zhaxybayeva et al. 2009; Nesbø et al. 2015). Some of these habitats can be very different, e.g. marine hydrothermal vents and deep subsurface oil reservoirs. It is however unclear, how habitat-range influences genome structure and content, levels of homologous recombination and HGT (and *vice versa*).

Here we shed light on these questions by analyzing multiple isolates of the Thermotogae genus *Thermosipho*. The isolates were obtained from various ecosystems across the globe (Table 1) and fall into 3 different lineages or species: *T. melanesiensis*, *T.africanus* and *T. affectus*. *T. melanesiensis* and *T. affectus* isolates were only obtained from hydrothermal vents from one specific geographical region, while *T. africanus* members have been obtained from a wide range of geographical and ecologically different environments (oil reservoirs, hydrothermal vents and terrestrial hot springs). This implies that the genus *Thermosipho* has specialist and generalist species, with the latter being present in a wider range of ecosystems.

Although the above observation may be partly due to sampling and cultivation bias, comparison with 16S rRNA genes from environmental samples (Dahle et al. 2008; Nakagawa:2006jr; Stevenson et al. 2011; Smith et al. 2017) also supports this view, where the

bioRxiv preprint doi: https://doi.org/10.1101/106989; this version posted February 8, 2017. The copyright holder for this preprint (which was not certified by peer review) is the author/funder, who has granted bioRxiv a license to display the preprint in perpetuity. It is made available under aCC-BY-NC-ND 4.0 International license.

two lineages restricted to hydrothermal vents from a distinct branch in the 16S rRNA tree (Figure 1). The fact that these lineages are restricted to hydrothermal vents and appear to have more limited geographic ranges, suggests that these are more specialized species in comparison to species found on the other 16S rRNA tree branch. Interestingly, in addition to oil reservoirs, *Thermosipho* sp. have also been detected in subsurface crustal fluids Smith et al., (2016) and their amplicon 16S rRNA sequences align best with species of the "generalist" branch of the 16S rRNA tree (Data not shown). These results suggest that *Thermosipho* lineages are widespread in the subsurface and not restricted to oil reservoirs or hydrothermal vents.

Another representative of the *Thermotogae* species, where ecology is suggested to be important for differentiation, is *Thermotoga maritima*. For this lineage, similar ecology was found to be more important than close geographical distance to maintain highly similar genomes through extensive gene flow (Nesbø et al. 2015); genomes from the same type of environment (i.e. oil reservoir or marine vent) were more similar to each other than geographically close genomes from different types of environments (Nesbø et al. 2015).

As in *T. maritima* we found that within *Thermosipho* sp. gene flow appears to be important for the maintenance of the three distinct lineages or species, as we observe high levels of recombination within the three lineages investigated. However, we also see a clear differentiation of the three species with no recombination between lineages. These results were further supported by the pangenome analysis of the genus *Thermosipho* (Figure 3B). Each lineage, or species, contained a set of species-specific genes that were at best only distantly related to genes in the other lineages. These genes mark the species boundaries and possibly contribute to niche differentiation between the different *Thermosipho* species. This was especially clear from the analysis of genes involved in carbohydrate and coenzyme metabolism (COG category G and H).

bioRxiv preprint doi: https://doi.org/10.1101/106989; this version posted February 8, 2017. The copyright holder for this preprint (which was not certified by peer review) is the author/funder, who has granted bioRxiv a license to display the preprint in perpetuity. It is made available under aCC-BY-NC-ND 4.0 International license.

These carbohydrate and coenzyme metabolism genes are important for energy production and central metabolism and could play a role in the niche differentiation of the *Thermosipho* species. For instance, the *T. affectus* genome contains several genes with a dependency for vitamin B12 (e.g. B12 dependent methionine synthase, ribonucleotide reductase Class II)(Swithers et al. 2011). However, the absence of most genes needed for the corrinoid synthesis (needed for de-novo Vitamin B12 synthesis) (Coenyzme category) in *T. affectus* suggests that this organism can only rely on the recovery of Vitamin B12 precursor molecules (Supplementary materials Figure S4). It is unclear how this affects its physiology and ecology. It will however, certainly affect the type of environments it can inhabit and its role and interaction with other species in the communities they are part of. Likewise, *T. africanus* has more genes involved in carbohydrate metabolism, which suggests that this species is more diverse with respect to which carbohydrate molecules it can utilize. This seems to be in line with the literature, (Podosokorskaya et al. 2014; Dipasquale et al. 2014) and it could be partly responsible for its wider distribution in different ecosystems.

It is notable, that the species with the largest, and also most variable genomes, have the widest distribution, both geographically and ecologically. However, the difference in genomic variation *within* three lineages is probably also partly due of the fact that the *T. africanus* isolates were sampled from three different geographically separated populations, while the *T. melanesiensis* isolates all originated from a single population sampled at the same time from the same ecosystem. The *T. affectus* genomes originated from two geographically close sites and show intermediate levels of variation (Table 1). These results suggest that isolation by distance is an important factor for differentiation in *Thermosipho* sp., as found in other thermophiles {Mino:2017gj}. However, since *T. affectus* and *T. melanesiensis* have not been detected at other locations than the isolation sites described here, this may be an entirely academic question for these species.

bioRxiv preprint doi: https://doi.org/10.1101/106989; this version posted February 8, 2017. The copyright holder for this preprint (which was not certified by peer review) is the author/funder, who has granted bioRxiv a license to display the preprint in perpetuity. It is made available under aCC-BY-NC-ND 4.0 International license.

642

643 *Dealing with invasive DNA*

644 Phages and transposons are known vectors of "foreign" DNA with possible deleterious
645 effects, therefore limiting their integration and activity is an essential survival strategy for
646 many, if not all, bacterial species (Stern & Sorek 2011). Several mobile elements were
647 detected in the *Thermosipho* genomes. For instance, *T. africanus* TCF52B carries 18 copies of
648 a transposase (COG2801). Moreover, one *T. africanus* (H17ap60334), one *T. affectus*
649 (BI1074) and all the *T. melanesiensis* strains have a prophage integrated into their genomes
650 (Haverkamp et al., unpublished). The presence of prophages in Thermotogales species has
651 earlier only been described in the thermophile *Marinitoga piezophila*, and analysis of the
652 phage (named MPV1) genome suggested it has played an important role as a HGT vector
653 (Lossouarn et al. 2015). A large fraction of its genes show a close phylogenetic relationship
654 with Firmicutes, the Thermotogae's main HGT partner (Zhaxybayeva et al. 2009). The
655 identification of multiple phages in *Thermosipho* genomes further supports the idea that
656 phage particles could be the general intermediates in gene flow within and between species in
657 the subsurface (Labonté et al. 2015).

658 Nonetheless, phages can be detrimental for prokaryotic cells such as *Thermosipho*, so
659 mechanisms are in place in this genus to intercept incoming foreign DNA. These mechanisms
660 consist of the RM and the CRISPR-cas system, that both play a role in intercepting invasive
661 DNA. The presence of CRISPR-cas genes, which are involved in prokaryotic immunity,
662 among the species- and strain specific genes is no surprise since they have been identified
663 before on mobile elements such as transposons and phages (Sebaihia et al. 2006; Seed et al.
664 2013). One example of this is a mobile element in *T. africanus* TCF52B flanked by
665 transposase recognition sites, which contains CRISPR-cas genes (Nesbø et al. 2009). This

bioRxiv preprint doi: https://doi.org/10.1101/106989; this version posted February 8, 2017. The copyright holder for this preprint (which was not certified by peer review) is the author/funder, who has granted bioRxiv a license to display the preprint in perpetuity. It is made available under aCC-BY-NC-ND 4.0 International license.

666 further indicates that mobile elements are not always deleterious for the receiver, but they can
667 be a source of novel beneficial genetic material.

668 The comparative genome analysis shows that there are clear differences between the
669 three *Thermosipho* species in the completeness of the systems, which may have implications
670 for acquiring novel DNA via HGT or recombination. For instance, all isolates have the
671 CRISPR-cas system, but the number of genes per genome related to this system differs, and in
672 *T. africanus* H17ap60334 the CRISPR-cas system may not be complete enough to be
673 functional. On the other hand, in contrast to the two other species the RM system is
674 incomplete in *T. affectus* species and likely not functional, indicating that *T. affectus* isolates
675 only rely on the CRISPR-cas system for defense against foreign DNA.

676 The lack of a working RM system was confirmed through PacBio sequencing of
677 strains *T. affectus* BI1063 and *T. affectus* BI1070 that showed no methylation. Pacbio
678 sequencing of *T. melanesiensis* BI431 revealed a methylated genome supporting the presence
679 of a working RM system. The genome of the isolate and the integrated prophage were
680 methylated. One of the RM systems detected in *T. melanesiensis* BI431 is located in the
681 integrated prophage, but it is not the only system that is active. Both host and prophage
682 methylases are expressed and methylation is detected at sites specific for those methylases
683 (Table 4). The presence and activity of a methylase in the prophage genome is a well know
684 evasive mechanism deployed by phages to escape the host RM system (Stern & Sorek 2011).

685 That the host RM system is active suggests that *T. melanesiensis* strains repeatedly
686 encounter mobile DNA / phages in their natural environment. This is also suggested by the
687 low similarity of one of the CRISPR array spacers with the prophage genome, which implies
688 that considerable divergence has occurred since the creation of the spacer and the integration
689 of the detected prophage. If the sequence match had been perfect, it would have been likely
690 that the prophage could not have integrated since the CRISPR machinery would have stopped

bioRxiv preprint doi: https://doi.org/10.1101/106989; this version posted February 8, 2017. The copyright holder for this preprint (which was not certified by peer review) is the author/funder, who has granted bioRxiv a license to display the preprint in perpetuity. It is made available under aCC-BY-NC-ND 4.0 International license.

691 it at the door. Another interesting observation was the presence of a spacer, in both *T.*
692 *africanus* strains TCF52B and H17ap60334, similar but not identical to a spacer in the
693 genome of *Pseudothermotoga elfii* DSM 9442. This suggests the presence in the subsurface
694 of a broad range phage infecting both species.
695 Taken together, the observations of the diversity of CRISPR-cas systems, RM
696 systems, and mobile elements (i.e. prophages and transposons) in *Thermosipho*, indicate that
697 mobile DNA, such as phages and transposons, frequently interact with these bacterial
698 genomes in the subsurface. Recently, it was shown that phages are dominant players in the
699 subsurface realm, influencing ecosystem function by interacting with their prokaryotic hosts
700 (Engelhardt et al. 2015). It also implies that mobile DNA plays an important role in shaping
701 *Thermosipho* populations and species in the subsurface.
702
703 *Conclusions*
704 Here we compared the genomes of fifteen different *Thermosipho* isolates and found that they
705 belong to three clearly separated lineages or species: *T. affectus*, *T. africanus* and *T.*
706 *melanesiensis*. Recombination detection showed very little interspecies gene flow, but high
707 intraspecies gene flow. This finding was supported by the presence of large groups of species-
708 specific gene sets, reflecting the metabolic differences between the species. The species-
709 specific genes sets may further be responsible for differences in distribution of these species
710 in various ecosystems such as hydrothermal vents and petroleum reservoirs. Our observations
711 suggest that genome similarity in this genus decreases with increasing distance. However,
712 additional genome sequences of *Thermosipho* isolates from different locations and lineages
713 within this genus are needed in order to confirm this. Our analysis also revealed that the
714 presence of prophage elements is not uncommon in these thermophiles. It also showed that
715 each of the species has a different capacity for dealing with incoming DNA from phages and

bioRxiv preprint doi: https://doi.org/10.1101/106989; this version posted February 8, 2017. The copyright holder for this preprint (which was not certified by peer review) is the author/funder, who has granted bioRxiv a license to display the preprint in perpetuity. It is made available under aCC-BY-NC-ND 4.0 International license.

716 other mobile elements, which also affects intra-species gene flow. The presence of multiple
717 prophage elements in several *Thermosipho* isolates suggests that the high fraction of
718 horizontally acquired genes is possibly due to ongoing warfare between bacteria and phages
719 in the subsurface. Finally, the presence of similar CRISPR spacers, in multiple species and
720 isolates indicates that phages in the subsurface have broad host ranges allowing for inter-
721 species gene flow. That could ultimately explain why many genes in Thermotogales genomes
722 show high similarity with genes found in Archaea or Firmicutes genomes.
723

bioRxiv preprint doi: https://doi.org/10.1101/106989; this version posted February 8, 2017. The copyright holder for this preprint (which was not certified by peer review) is the author/funder, who has granted bioRxiv a license to display the preprint in perpetuity. It is made available under aCC-BY-NC-ND 4.0 International license.

724 **Acknowledgements**

725 The work of THAH and CLN, was supported was funded by the Norwegian Research
726 Council (award 180444/V40). JL and CG were supported by Agence Nationale de la
727 Recherche (ANR) (ANR-12-BSV3-OO23-01). OAP and IVK were supported by the Russian
728 Science Foundation (RSF) grant # 16-14-00121. We thank the Norwegian Sequencing Centre
729 for sequencing and support with the bioinformatics analysis. We thank Ifremer and chief
730 scientists of the French oceanographic cruises “Biolau” (1989), “Marvel” (1997) and “Atos”
731 (2001). Strains are available under request at the ‘Souchothèque de Bretagne’ (catalogue
732 LMBE) culture collection (http://www.univ.brest.fr/souchoteque/collection+LM2E).

733

734

bioRxiv preprint doi: https://doi.org/10.1101/106989; this version posted February 8, 2017. The copyright holder for this preprint (which was not certified by peer review) is the author/funder, who has granted bioRxiv a license to display the preprint in perpetuity. It is made available under aCC-BY-NC-ND 4.0 International license.

References

Alikhan N-F, Petty NK, Ben Zakour NL, Beatson SA. 2011. BLAST Ring Image Generator (BRIG): simple prokaryote genome comparisons. BMC Genomics. 12:402. doi: 10.1186/1471-2164-12-402.

Antoine E et al. 1997. *Thermosipho melanesiensis* sp. nov., a new thermophilic anaerobic bacterium belonging to the order *Thermotogales*, isolated from deep-sea hydrothermal vents in the southwestern Pacific Ocean. Int. J. Syst. Bacteriol. 47:1118–1123. doi: 10.1099/00207713-47-4-1118.

Archibald JM, Roger AJ. 2002a. Gene conversion and the evolution of euryarchaeal chaperonins: a maximum likelihood-based method for detecting conflicting phylogenetic signals. J Mol Evol. 55:232–245. doi: 10.1007/s00239-002-2321-5.

Archibald JM, Roger AJ. 2002b. Gene duplication and gene conversion shape the evolution of archaeal chaperonins. Journal of Molecular Biology. 316:1041–1050. doi: 10.1006/jmbi.2002.5409.

Bankevich A et al. 2012. SPAdes: a new genome assembly algorithm and its applications to single-cell sequencing. Journal of Computational Biology. 19:455–477. doi: 10.1089/cmb.2012.0021.

Cady KC, O'Toole GA. 2011. Non-identity-mediated CRISPR-bacteriophage interaction mediated via the Csy and Cas3 proteins. J Bacteriol. 193:3433–3445. doi: 10.1128/JB.01411-10.

Camacho C et al. 2009. BLAST+: architecture and applications. BMC Bioinformatics. 10:421. doi: 10.1186/1471-2105-10-421.

Charbonnier F, Erauso G, Barbeyron T, Prieur D, Forterre P. 1992. Evidence that a plasmid from a hyperthermophilic archaebacterium is relaxed at physiological temperatures. J Bacteriol. 174:6103–6108.

Dahle H, Garshol F, Madsen M, Birkeland N-K. 2008. Microbial community structure analysis of produced water from a high-temperature North Sea oil-field. Antonie van Leeuwenhoek. 93:37–49. doi: 10.1007/s10482-007-9177-z.

Darmon E, Leach DRF. 2014. Bacterial genome instability. Microbiol. Mol. Biol. Rev. 78:1–39. doi: 10.1128/MMBR.00035-13.

Darriba D, Taboada GL, Doallo R, Posada D. 2012. jModelTest 2: more models, new heuristics and parallel computing. Nat Meth. 9:772–772. doi: 10.1038/nmeth.2109.

Dipasquale L, Romano I, Picariello G, Calandrelli V, Lama L. 2014. Characterization of a native cellulase activity from an anaerobic thermophilic hydrogen-producing bacterium *Thermosipho* sp. strain 3. Ann Microbiol. 64:1493–1503. doi: 10.1007/s13213-013-0792-9.

Engelhardt T, Orsi WD, Jørgensen BB. 2015. Viral activities and life cycles in deep subseafloor sediments. Environ Microbiol Rep. 7:868–873. doi: 10.1111/1758-2229.12316.

Enright AJ, Van Dongen S, Ouzounis CA. 2002. An efficient algorithm for large-scale

bioRxiv preprint doi: https://doi.org/10.1101/106989; this version posted February 8, 2017. The copyright holder for this preprint (which was not certified by peer review) is the author/funder, who has granted bioRxiv a license to display the preprint in perpetuity. It is made available under aCC-BY-NC-ND 4.0 International license.

773 detection of protein families. Nucleic Acids Res. 30:1575–1584. doi: 10.1093/nar/30.7.1575.

774 Geslin C et al. 2003. PAV1, the first virus-like particle isolated from a hyperthermophilic
775 euryarchaeote, "*Pyrococcus abyssi*". J Bacteriol. 185:3888–3894. doi:
776 10.1128/JB.185.13.3888–3894.2003.

777 Goldfarb T et al. 2015. BREX is a novel phage resistance system widespread in microbial
778 genomes. EMBO J. 34:169–183. doi: 10.15252/embj.201489455.

779 Goris J et al. 2007. DNA-DNA hybridization values and their relationship to whole-genome
780 sequence similarities. Int J Syst Evol Microbiol. 57:81–91. doi: 10.1099/ijs.0.64483-0.

781 Grissa I, Vergnaud G, Pourcel C. 2007. CRISPRFinder: a web tool to identify clustered
782 regularly interspaced short palindromic repeats. Nucleic Acids Res. 35:W52–7. doi:
783 10.1093/nar/gkm360.

784 Hunt M et al. 2013. REAPR: a universal tool for genome assembly evaluation. Genome Biol.
785 14:R47. doi: 10.1186/gb-2013-14-5-r47.

786 Huson DH, Bryant D. 2006. Application of phylogenetic networks in evolutionary studies.
787 Molecular Biology and Evolution. 23:254–267. doi: 10.1093/molbev/msj030.

788 Koonin EV. 2015. The turbulent network dynamics of microbial evolution and the statistical
789 tree of life. J Mol Evol. 80:244–250. doi: 10.1007/s00239-015-9679-7.

790 Labonté JM et al. 2015. Single cell genomics indicates horizontal gene transfer and viral
791 infections in a deep subsurface Firmicutes population. Front Microbiol. 6:349. doi:
792 10.3389/fmicb.2015.00349.

793 Laing C et al. 2010. Pan-genome sequence analysis using Panseq: an online tool for the rapid
794 analysis of core and accessory genomic regions. BMC Bioinformatics. 11:461. doi:
795 10.1186/1471-2105-11-461.

796 Lawrence JG, Retchless AC. 2009. The interplay of homologous recombination and
797 horizontal gene transfer in bacterial speciation. In: Horizontal gene transfer: genomes in
798 flux.Vol. 532 pp. 29–53. doi: 10.1007/978-1-60327-853-9_3.

799 Li H et al. 2009. The sequence alignment/map format and SAMtools. Bioinformatics.
800 25:2078–2079. doi: 10.1093/bioinformatics/btp352.

801 Li H, Durbin R. 2009. Fast and accurate short read alignment with Burrows-Wheeler
802 transform. Bioinformatics. 25:1754–1760. doi: 10.1093/bioinformatics/btp324.

803 Lossouarn J et al. 2015. 'Ménage à trois': a selfish genetic element uses a virus to propagate
804 within Thermotogales. Environ. Microbiol. 17:3278–3288. doi: 10.1111/1462-2920.12783.

805 Makarova KS et al. 2015. An updated evolutionary classification of CRISPR-Cas systems.
806 Nat Rev Micro. 13:722–736. doi: 10.1038/nrmicro3569.

807 Makarova KS, Wolf YI, Snir S, Koonin EV. 2011. Defense islands in bacterial and archaeal
808 genomes and prediction of novel defense systems. J Bacteriol. 193:6039–6056. doi:
809 10.1128/JB.05535-11.

bioRxiv preprint doi: https://doi.org/10.1101/106989; this version posted February 8, 2017. The copyright holder for this preprint (which was not certified by peer review) is the author/funder, who has granted bioRxiv a license to display the preprint in perpetuity. It is made available under aCC-BY-NC-ND 4.0 International license.

Margulies M et al. 2005. Genome sequencing in microfabricated high-density picolitre reactors. Nature. 437:376–380. doi: 10.1038/nature03959.

Markowitz VM et al. 2009. IMG ER: a system for microbial genome annotation expert review and curation. Bioinformatics. 25:2271–2278. doi: 10.1093/bioinformatics/btp393.

Mukherjee S, Sengupta S. 2015. Riboswitch Scanner: an efficient pHMM-based web-server to detect riboswitches in genomic sequences. Bioinformatics. 32:776–778. doi: 10.1093/bioinformatics/btv640.

Nei M, Kumar S. 2000. *Molecular evolution and phylogenetics*. Oxford University Press: New York.

Nelson KE et al. 1999. Evidence for lateral gene transfer between Archaea and bacteria from genome sequence of *Thermotoga maritima*. Nature. 399:323–329. doi: 10.1038/20601.

Nesbø CL et al. 2015. Evidence for extensive gene flow and *Thermotoga* subpopulations in subsurface and marine environments. ISME J. 9:1532–1542. doi: 10.1038/ismej.2014.238.

Nesbø CL et al. 2009. The genome of *Thermosipho africanus* TCF52B: lateral genetic connections to the *Firmicutes* and *Archaea*. J Bacteriol. 191:1974–1978. doi: 10.1128/JB.01448-08.

Nesbø CL, Nelson KE, Doolittle WF. 2002. Suppressive subtractive hybridization detects extensive genomic diversity in *Thermotoga maritima*. J Bacteriol. 184:4475–4488. doi: 10.1128/JB.184.16.4475-4488.2002.

Overbeek R et al. 2013. The SEED and the Rapid Annotation of microbial genomes using Subsystems Technology (RAST). Nucleic Acids Res. 42:D206–D214. doi: 10.1093/nar/gkt1226.

Podosokorskaya OA et al. 2014. *Thermosipho activus* sp. nov., a thermophilic, anaerobic, hydrolytic bacterium isolated from a deep-sea sample. Int J Syst Evol Microbiol. 64:3307–3313. doi: 10.1099/ijs.0.063156-0.

Podosokorskaya OA, Kublanov IV, Reysenbach A-L, Kolganova TV, Bonch-Osmolovskaya EA. 2011. *Thermosipho affectus* sp. nov., a thermophilic, anaerobic, cellulolytic bacterium isolated from a Mid-Atlantic Ridge hydrothermal vent. Int J Syst Evol Microbiol. 61:1160–1164. doi: 10.1099/ijs.0.025197-0.

Quast C et al. 2013. The SILVA ribosomal RNA gene database project: improved data processing and web-based tools. Nucleic Acids Res. 41:D590–6. doi: 10.1093/nar/gks1219.

Rice P, Longden I, Bleasby A. 2000. EMBOSS: the European Molecular Biology Open Software Suite. Trends Genet. 16:276–277.

Richter M, Rosselló-Mora R. 2009. Shifting the genomic gold standard for the prokaryotic species definition. Proc Natl Acad Sci U S A. 106:19126–19131. doi: 10.1073/pnas.0906412106.

Roberts RJ, Vincze T, Posfai J, Macelis D. 2010. REBASE--a database for DNA restriction and modification: enzymes, genes and genomes. Nucleic Acids Res. 38:D234–6. doi:

bioRxiv preprint doi: https://doi.org/10.1101/106989; this version posted February 8, 2017. The copyright holder for this preprint (which was not certified by peer review) is the author/funder, who has granted bioRxiv a license to display the preprint in perpetuity. It is made available under aCC-BY-NC-ND 4.0 International license.

10.1093/nar/gkp874.

Roberts RJ, Vincze T, Posfai J, Macelis D. 2015. REBASE--a database for DNA restriction and modification: enzymes, genes and genomes. Nucleic Acids Res. 43:D298–9. doi: 10.1093/nar/gku1046.

Sebaihia M et al. 2006. The multidrug-resistant human pathogen *Clostridium difficile* has a highly mobile, mosaic genome. Nat Genet. 38:779–786. doi: 10.1038/ng1830.

Seed KD, Lazinski DW, Calderwood SB, Camilli A. 2013. A bacteriophage encodes its own CRISPR/Cas adaptive response to evade host innate immunity. Nature. 494:489–491. doi: 10.1038/nature11927.

Smith AR, Fisk MR, Thurber AR, Flores GE. 2017. Deep Crustal Communities of the Juan de Fuca Ridge Are Governed by Mineralogy. Geomicrobiology journal. 34:147–156. doi: 10.1080/01490451.2016.1155001.

Stern A, Sorek R. 2011. The phage-host arms race: shaping the evolution of microbes. Bioessays. 33:43–51. doi: 10.1002/bies.201000071.

Stevenson BS et al. 2011. Microbial communities in bulk fluids and biofilms of an oil facility have similar composition but different structure. Environ. Microbiol. 13:1078–1090. doi: 10.1111/j.1462-2920.2010.02413.x.

Swithers KS et al. 2011. Vitamin B(12) synthesis and salvage pathways were acquired by horizontal gene transfer to the *Thermotogales*. Genome Biology and Evolution. 4:730–739. doi: 10.1093/gbe/evs057.

Swofford DL. 2002. *PAUP*: Phylogenetic analysis using parsimony (*and other methods). v.4.0b10*. Sinauer & Associates: Sunderland, Massachusetts.

Takai K, Horikoshi K. 2000. *Thermosipho japonicus* sp. nov., an extremely thermophilic bacterium isolated from a deep-sea hydrothermal vent in Japan. Extremophiles. 4:9–17.

Takeuchi N, Kaneko K, Koonin EV. 2014. Horizontal gene transfer can rescue prokaryotes from Muller's Ratchet: benefit of DNA from dead cells and population Subdivision. G3: Genes| Genomes| Genetics. 4:325–339. doi: 10.1534/g3.113.009845/-/DC1.

Tamura K, Stecher G, Peterson D, Filipski A, Kumar S. 2013. MEGA6: Molecular Evolutionary Genetics Analysis Version 6.0. Molecular Biology and Evolution. 30:2725–2729. doi: 10.1093/molbev/mst197.

Thorvaldsdottir H, Robinson JT, Mesirov JP. 2013. Integrative Genomics Viewer (IGV): high-performance genomics data visualization and exploration. Briefings in Bioinformatics. 14:178–192. doi: 10.1093/bib/bbs017.

Vasu K, Nagaraja V. 2013. Diverse functions of restriction-modification systems in addition to cellular defense. Microbiol. Mol. Biol. Rev. 77:53–72. doi: 10.1128/MMBR.00044-12.

Weinberger AD, Wolf YI, Lobkovsky AE, Gilmore MS, Koonin EV. 2012. Viral diversity threshold for adaptive immunity in prokaryotes. MBio. 3:e00456–12. doi: 10.1128/mBio.00456-12.

bioRxiv preprint doi: https://doi.org/10.1101/106989; this version posted February 8, 2017. The copyright holder for this preprint (which was not certified by peer review) is the author/funder, who has granted bioRxiv a license to display the preprint in perpetuity. It is made available under aCC-BY-NC-ND 4.0 International license.

886 Westra ER et al. 2012. The CRISPRs, they are a-changin': how prokaryotes generate adaptive
887 immunity. Annu. Rev. Genet. 46:311–339. doi: 10.1146/annurev-genet-110711-155447.

888 Xu Z, Han D, Cao J, Saini U. 2011. Cloning and characterization of the TneDI restriction:
889 modification system of *Thermotoga neapolitana*. Extremophiles. 15:665–672. doi:
890 10.1007/s00792-011-0397-9.

891 Yin Y et al. 2012. dbCAN: a web resource for automated carbohydrate-active enzyme
892 annotation. Nucleic Acids Res. 40:W445–W451. doi: 10.1093/nar/gks479.

893 Zerbino DR, Birney E. 2008. Velvet: algorithms for de novo short read assembly using de
894 Bruijn graphs. Genome Research. 18:821–829. doi: 10.1101/gr.074492.107.

895 Zhaxybayeva O et al. 2009. On the chimeric nature, thermophilic origin, and phylogenetic
896 placement of the *Thermotogales*. Proc Natl Acad Sci U S A. 106:5865–5870. doi:
897 10.1073/pnas.0901260106.

898 Zhu Q, Kosoy M, Dittmar K. 2014. HGTector: an automated method facilitating genome-
899 wide discovery of putative horizontal gene transfers. BMC Genomics. 15:717. doi:
900 10.1186/1471-2164-15-717.

901

902

903

Tables

Table 1: Overview of *Thermosipho* genomes used in this study.

T. genome	NCBI accession number	Nr of contigs [#]	Genome size (bp)	GC content (%)	Sequence technology	Genome coverage [§]	Isolation source	References
T. melanesiensis BI429*[&]	NC_009616	1	1.915.238	31.4	454 / Sanger	-	Gills of mussel, Deep-sea H. vent, Pacific Ocean, Lau Basin	Antoine et al., 1997 Zhaxybayeva et al., 2009
T. melanesiensis 430[&]	JYCX00000000	4	1.906.053	31.5	MiSeq	243[M]	Gills of gastropod Deep-sea H.	
T. melanesiensis 431[&]	CP007389	1	1.915.344	31.4	Pacbio /MiSeq	34[P]/223[M]	Sample of active chimney	this study
T. melanesiensis 432[&]	JYCY00000000	21	1.890.294	32.6	MiSeq	230[M]	Sample of active chimney	this study
T. melanesiensis 433[&]	JYCZ00000000	21	1.890.575	32.6	MiSeq	256[M]	Gills of a mussel	
T. melanesiensis 434[&]	JYDA00000000	22	1.892.506	32.7	MiSeq	234[M]		
T. melanesiensis 487[&]	JYDB00000000	21	1.890.479	32.6	MiSeq	239[M]	Sample of active chimney	
T. *affectus* 1063[%]	CP007223	1	1.766.633	31.5	Pacbio /MiSeq	38[P]/304[M]	Deep sea H. vent, Atlantic ocean	Wery et al., 2002
T. *affectus* 1070[%]	CP007121	1		31.5	Pacbio /MiSeq	37[P]/257[M]	Menez-Gwen hydrothermal field	this study
T. *affectus* 1074[%]	LBEX00000000	20	1.788.307	33.3	MiSeq	258[M]	Menez-Gwen hydrothermal field	this study
T. *affectus* ik275mar	LBFC00000000	27	1.771.018	32.6	MiSeq	256[M]	Rainbow H.vent field	Podosokorskaya et al., 2011
T. *affectus* sp. 1223[∞]	LBEY00000000	39	1.767.555	32.1	MiSeq	226[M]	Rainbow H.vent field	this study
T. africanus ob7	?	23	1.933435	32.7	Ion Torrent	-	Tadjoura gulf Hydrothermal springs	Huber et al,.1989
T. africanus H17ap60334	AJIP0100000	49	2.083.551	29.9	454 / Sanger	310	production water Hibernia oil platform	this study
T. africanus TCF52B*	NC_011653	1	2.016.657	30.8	Sanger	-	production water Troll C oil platform, North Sea	Dahle et al., 2008 Nesbø et al., 2009

[*] Not sequenced during this study

[&] Strains 429 to 487 isolated during Oceanographic cruise Biolau: Pacific Ocean, Lau Basin, Deep-sea Hydrothermal vent .

bioRxiv preprint doi: https://doi.org/10.1101/106989; this version posted February 8, 2017. The copyright holder for this preprint (which was not certified by peer review) is the author/funder, who has granted bioRxiv a license to display the preprint in perpetuity. It is made available under aCC-BY-NC-ND 4.0 International license.

908 [%] Strains 1063 to 1074 isolated during Oceanographic cruise Marvel: Atlantic ocean, Menez Gwen, Deep-sea Hydrothermal vent

909 [∞] Isolated during Oceanographic cruise Atos, Atlantic ocean, Rainbow, Deep sea Hydrothermal vent.

910 [#] Genomes with 1 contig were closed

911 [§ M]: MiSeq sequencing; [P]: Pacbio RSII sequencing;

912

bioRxiv preprint doi: https://doi.org/10.1101/106989; this version posted February 8, 2017. The copyright holder for this preprint (which was not certified by peer review) is the author/funder, who has granted bioRxiv a license to display the preprint in perpetuity. It is made available under aCC-BY-NC-ND 4.0 International license.

913 **Table 2.** Overview of genome content with a focus on mobile DNA defence systems and mobile elements

Genome	Closed	ORFs	Species-specific ORFs	Strain specific ORFs	Putative HGT ORFs	Defence genes	CRISPR arrays	Prophage present	Prophage ORFs
T. melanesiensis BI429	Y	1879	424	33	80	37	5	Yes	49
T. melanesiensis 430		1831	426	0	81	36	5	Yes	51
T. melanesiensis 431	Y	1868	422	4	83	36	5	Yes	53
T. melanesiensis 432		1827	424	0	78	36	5	Yes	52
T. melanesiensis 433		1832	424	0	82	36	5	Yes	51
T. melanesiensis 434		1833	425	0	81	36	5	Yes	52
T. melanesiensis 487		1828	424	0	79	36	5	Yes	52
T. affectus 1063	Y	1706	349	11	66	35	4		
T. affectus 1070	Y	1765	351	43	71	35	4		
T. affectus 1074		1756	353	47	73	36	5	Yes	77
T. affectus ik275mar		1720	348	17	71	34	5		
T. affectus 1223		1726	349	68	76	32	5		
T. africanus ob7		1902	638	63	83	30	6		
T. africanus H17ap60334		1982	656	169	116	28	6	Yes	48
T. africanus TCF52B	Y	1954	657	64	77	38	12		

914

bioRxiv preprint doi: https://doi.org/10.1101/106989; this version posted February 8, 2017. The copyright holder for this preprint (which was not certified by peer review) is the author/funder, who has granted bioRxiv a license to display the preprint in perpetuity. It is made available under aCC-BY-NC-ND 4.0 International license.

915 [#]: Each genome is used as a reference therefore species-specific orfs can show variations.
916

bioRxiv preprint doi: https://doi.org/10.1101/106989; this version posted February 8, 2017. The copyright holder for this preprint (which was not certified by peer review) is the author/funder, who has granted bioRxiv a license to display the preprint in perpetuity. It is made available under aCC-BY-NC-ND 4.0 International license.

Table 3. Unique gene counts per genome. Counts were obtained at the IMG database using the phylogenetic profile tool using single genes. The genes of each genome were compared to the genes of all other genomes to identify genes without homologs in the reference genome, with a minimum similarity of 70% and pseudogenes were excluded.

Genome	Unique genes (n)	hypothetical proteins	Block >= 4 genes	Genes per block	Block CDS Ids	Mobile Element related function
T. melanesiensis						
BI429	33	29	0			
BI430	0	0	0			
BI431	4	1	0			
BI432	0	0	0			
BI433	0	0	0			
BI434	0	0	0			
BI487	0	0	0			
T. affectus						
BI1063	11	3	1	10	BG95_04145 - BG95_04190	
BI1070	43	34	1	11	Y592_04200 - Y592_04260	
BI1074	47	30	3	6	XO08_04050 - XO08_04075	
				31	XO08_07660 - XO08_07830	Putative Prophage
				8	XO08_07895 - XO08_07930	
BI1223	68	29	6	7	XO09_00565 - XO09_00600	CRISPR/Cas system
				8	XO09_03190 - XO09_03225	
				11	XO09_04035 - XO09_04085	
				8	XO09_04140 - XO09_04175	
				15	XO09_04205 - XO09_04275	
				8	XO09_08625 - XO09_08665	

bioRxiv preprint doi: https://doi.org/10.1101/106989; this version posted February 8, 2017. The copyright holder for this preprint (which was not certified by peer review) is the author/funder, who has granted bioRxiv a license to display the preprint in perpetuity. It is made available under aCC-BY-NC-ND 4.0 International license.

ik275mar	17	7	1	11	XJ44_04105 - XJ44_04155	2 transposases
T. africanus						
H17ap60334	169	67	10	5	H17ap60334_01201 - H17ap60334_01226	
				6	H17ap60334_04767 - H17ap60334_04797	Prophage region
				19	H17ap60334_04812 - H17ap60334_04902	Prophage region
				7	H17ap60334_04967 - H17ap60334_04997	Prophage region
				6	H17ap60334_07553 - H17ap60334_07578	
				17	H17ap60334_07603 - H17ap60334_07683	
				31	H17ap60334_07703 - H17ap60334_07853	
				6	H17ap60334_09624 - H17ap60334_09649	CRISPR/Cas system
				6	H17ap60334_10649 - H17ap60334_10674	
				4	H17ap60334_11513 -H17ap60334_11528	
Ob7	63	14	4	6	Ob7_07340 - Ob7_07365	
				18	Ob7_07400 - Ob7_07485	
				4	Ob7_07685 - Ob7_07700	
				6	Ob7_09642 - Ob7_09667	
TCF52B	64	38	3	9	THA_741 - THA_749	
				10	THA_1252 THA_1261	Mobile element with CRISPR/Cas system
				5	THA_1949 - THA_1953	

921
922

bioRxiv preprint doi: https://doi.org/10.1101/106989; this version posted February 8, 2017. The copyright holder for this preprint (which was not certified by peer review) is the author/funder, who has granted bioRxiv a license to display the preprint in perpetuity. It is made available under aCC-BY-NC-ND 4.0 International license.

Table 4. Overview of modification and motif analysis for three *Thermosipho* strains using Pacbio sequencing. Modification and motif analysis was performed using the RS_modifcation_and_motif_analysis.1 pipeline using the SMRT sequencing subreads and as a reference the non-closed quiver polished HGAP assembly for each genome. Bases with m6A methylation were identified along the entire chromosome sequences of *Thermosipho melanesiensis* 431.

Strain	Methylase gene* (Type)	Motif	Modification type	Motifs in Genome	Fraction methylated motifs	mean score	Mean IPD# Ratio	Mean Coverage
T. melanesiensis BI431	BW47_01680 (II)	GATC	m6A	5446	0,99	72,6	4,60	48,3
	BW47_02200 (I)	RTAYNNNNNNTNNCG	m6A	520	0,95	70,6	5,13	48,0
	BW47_02200 (I)	CGNNANNNNNNRTAY	m6A	520	0,94	66,9	4,75	48,5
	BW47_07880§ (II)	CCGG	m4C	2968	0,71	45,8	3,63	49,1
	BW47_08940 (III)	CGCC	m4C	2462	0,62	44,6	3,07	52,3
T. affectus BI1063$		Not Clustered	Not applicable	3584808	0,09	37,4	na	81,2
T. affectus. BI1070$		CNNNTNCNNTAANATNG	modified base	72	0,50	41,3	2,60	39,9

*) Methylase genes are linked to the detected motif via the REBASE database predictions.
#) IPD: Inter Pulse Density
§) Methylase gene present in the detected prophage region.
$) Non-significant results

bioRxiv preprint doi: https://doi.org/10.1101/106989; this version posted February 8, 2017. The copyright holder for this preprint (which was not certified by peer review) is the author/funder, who has granted bioRxiv a license to display the preprint in perpetuity. It is made available under aCC-BY-NC-ND 4.0 International license.

Table 5. CRISPR array comparison of 15 *Thermosipho* genomes. CRISPR arrays were detected using CRISPRfinder (Grissa et al. 2007). Spacers were extracted and blasted against the own genome to determine if there were other similar sequences present in the genome. Most spacers that showed hits, matched other spacers found in one of the CRISPRarrays of the genome.

Genome	CRISPR arrays (*)	Average repeat length	Total nr spacers	average number of spacers[$]	average spacer length	total spacer length	Spacers with multiple blast hits against own genome[#]	Spacers with non spacer blast hits
T. melanesiensis BI429	5	30	94	18,8	38,96	3728	18	2
T. melanesiensis BI430	5	30	98	19,6	38,94	3882	18	2
T. melanesiensis BI431	5	30	98	19,6	38,94	3882	18	2
T. melanesiensis BI432	5	30	98	19,6	38,94	3882	18	2
T. melanesiensis BI433	5	30	98	19,6	38,94	3882	18	2
T. melanesiensis BI434	5	30	97	19,4	38,92	3840	18	2
T. melanesiensis BI487	5	30	98	19,6	38,94	3882	18	2
T. affectus BI1063	4	31,25	106	26,5	37,28	3900	9	0
T. affectus BI1070	4	31,5	107	26,75	37,31	3951	10	0
T. affectus BI1074	5	31,2	58	11,6	36,58	2134	2	0
T. affectus ik275mar	5	32,4	87	17,4	38,93	3315	7	1
T. affectus BI1223	4(1)	31,4	54	10,8	38,05	2002	2	0
T. africanus ob7	6(1)	28,9	106	15,1	39,33	4240	6	2
T. africanus H17ap60334	6(1)	28,9	189	27	40,75	7628	19	8
T. africanus TCF52B	12	30	321	26,7	38,73	12454	37	5

* number of questionable CRISPR arrays
[$] averaged per number of arrays
[#] mostly hits against highly similar spacers found in the genome.

bioRxiv preprint doi: https://doi.org/10.1101/106989; this version posted February 8, 2017. The copyright holder for this preprint (which was not certified by peer review) is the author/funder, who has granted bioRxiv a license to display the preprint in perpetuity. It is made available under aCC-BY-NC-ND 4.0 International license.

bioRxiv preprint doi: https://doi.org/10.1101/106989; this version posted February 8, 2017. The copyright holder for this preprint (which was not certified by peer review) is the author/funder, who has granted bioRxiv a license to display the preprint in perpetuity. It is made available under aCC-BY-NC-ND 4.0 International license.

940 ## Figure legends

941 **Figure 1.** Maximum Likelihood phylogeny of *Thermosipho* 16S rRNA sequences constructed
942 in conducted in MEGA6 (Tamura et al., 2013). The General Time Reversible (GTR) model
943 (G+I, 4 categories, (Nei & Kumar 2000)) was used. The tree with the highest log likelihood is
944 shown. The percentage of trees in which the associated taxa clustered together is shown next
945 to the branches. Initial tree(s) for the heuristic search were obtained by applying the
946 Neighbor-Joining method to a matrix of pairwise distances estimated using the Maximum
947 Composite Likelihood (MCL) approach. The tree is drawn to scale, with branch lengths
948 measured in the number of substitutions per site, bar indicates 0.05 substitutions per site. The
949 analysis involved 61 nucleotide sequences. All positions with less than 95% site coverage
950 were eliminated. That is, fewer than 5% alignment gaps, missing data, and ambiguous bases
951 were allowed at any position. There were a total of 1245 positions in the final dataset. The
952 phylogeny is rooted using 16S rRNA gene sequences of representative sequences from other
953 Thermotogae genera (*Defluviitoga*, *Fervidobacterium*, *Geotoga*, *Kosmotoga*, *Marinitoga*,
954 *Mesoaciditoga*, *Mesotoga*, *Oceanotoga*, *Petrotoga*, *Pseudothermotoga* and *Thermotoga*). All
955 non-*Thermosipho* Thermotogales formed an outgroup and were collapsed (Supplementary
956 figure S1 for the full phylogeny). *Thermosipho* sequences are colored based on the
957 environment of isolation. Sequences with bold fonts are whole genome sequences. Triangles
958 behind the sequence ID indicate genome not from this study. Circles behind sequence ID
959 indicate genome from this study.
960
961 **Figure 2**
962 Comparison of the *Thermosipho* genomes based on pairwise tetranucleotide frequency
963 correlation coefficients (TETRA). Dark blue indicate highly similar genomes, while red
964 indicate low similarity. The colored lines (black, green and blue) indicate to which

bioRxiv preprint doi: https://doi.org/10.1101/106989; this version posted February 8, 2017. The copyright holder for this preprint (which was not certified by peer review) is the author/funder, who has granted bioRxiv a license to display the preprint in perpetuity. It is made available under aCC-BY-NC-ND 4.0 International license.

965 *Thermosipho* lineage/species the strains belong. The heatmap was created in R-studio using
966 pairwise TETRA values calculated with the JSpeciesWS server (Richter et al., 2015).
967
968 **Figure 3**
969 A) Neighbor network of the 15 *Thermosipho* strains. The network is based SNP's in core
970 genome fragments that were present in all genomes with a minimum of 70% similarity. The
971 network was visualized in Splitstree using the NeighborNet algorithm (Huson and Bryant,
972 2006) from uncorrected distances. B) Fraction of genes shared between 15 *Thermosipho*
973 genomes. Data was generated at the IMG-database using pairwise Bidirectional Best
974 nSimScan Hits, with genes sharing 70% sequence identity and at least 70% coverage.
975 Percentages were calculated by dividing the number shared genes by the total number of
976 genes for the genome on the y-axis. The colored lines (black, green and blue) indicated which
977 strains belong to which *Thermosipho* lineage/species.
978
979 **Figure 4**
980 Comparison of average relative COG category gene counts for three *Thermosipho* species. **A)**
981 Complete genome COG category annotations. **B)** Species-specific genes COG annotations.
982 COG gene annotations for each genome were summarized per category and genome counts
983 were standardized using total COG annotation counts per genomes. For the complete genome
984 COG annotations, the Kruskal-wallis test was performed on standardized counts using the
985 species clusters as groups. Categories with significant differences (p-value <=0.01) between
986 the species are indicated with **. The standard error of relative category counts per species, is
987 indicated by the errors bars.
988
989 **Figure 5**

bioRxiv preprint doi: https://doi.org/10.1101/106989; this version posted February 8, 2017. The copyright holder for this preprint (which was not certified by peer review) is the author/funder, who has granted bioRxiv a license to display the preprint in perpetuity. It is made available under aCC-BY-NC-ND 4.0 International license.

990 Mobile DNA defense related COG annotation counts for 15 *Thermosipho* isolates. A total of
991 38 COGs were identified using a list of COGs related to defense genes (Makarova et al.
992 2011). The counts of the identified COGs were summarized into three groups: Restriction-
993 modification systems COGs, CRISPR-cas associated COGs, and other COGs. The strains are
994 grouped per *Thermosipho* species.
995

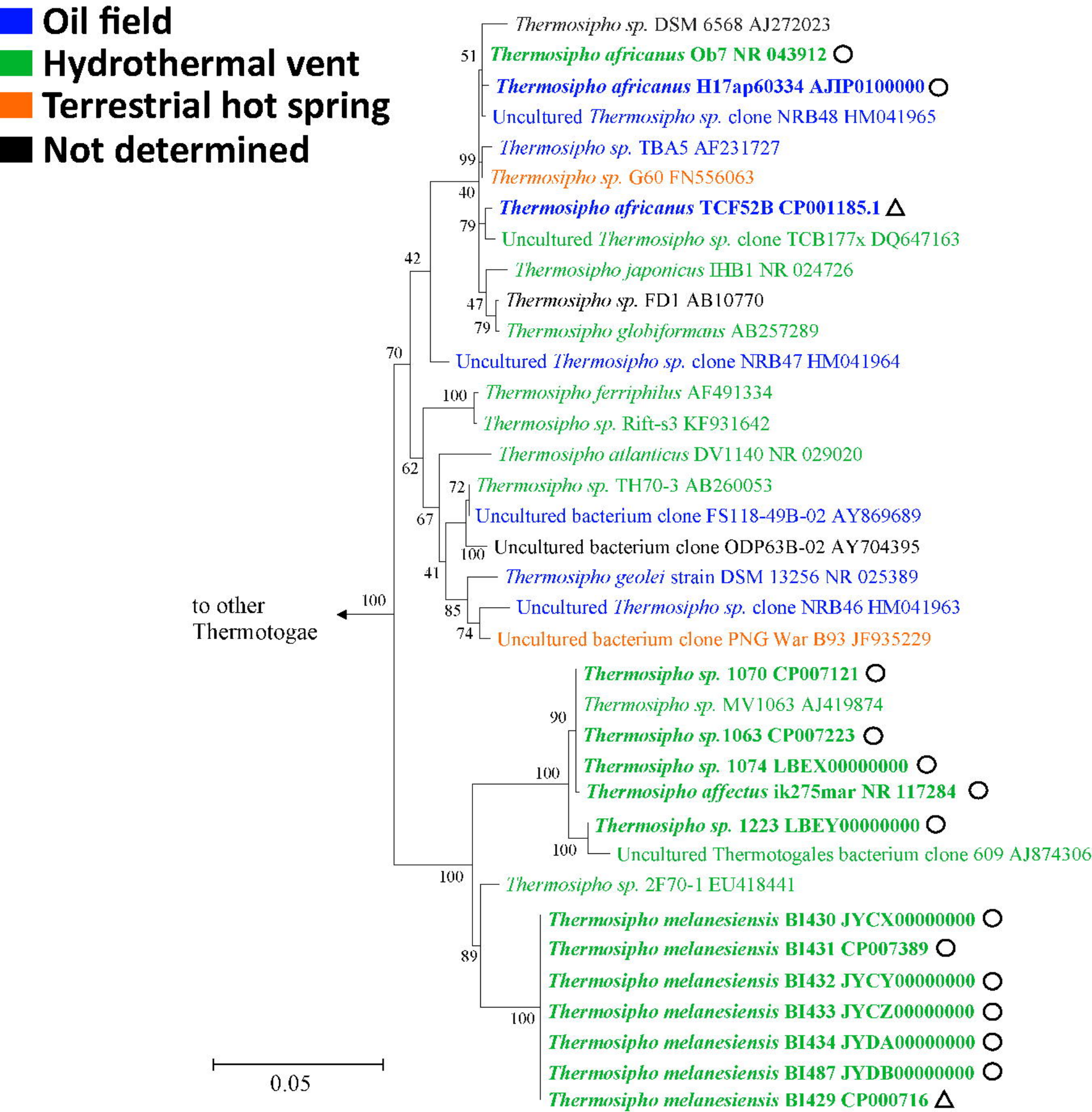
Oil field
Hydrothermal vent
Terrestrial hot spring
Not determined
Thermosipho sp. DSM 6568 AJ272023
Thermosipho africanus Ob7 NR 043912
Thermosipho africanus H17ap60334 AJIP0100000
Uncultured Thermosipho sp. clone NRB48 HM041965
Thermosipho sp. TBA5 AF231727
Thermosipho sp. G60 FN556063
Thermosipho africanus TCF52B CP001185.1
Uncultured Thermosipho sp. clone TCB177x DQ647163
Thermosipho japonicus IHB1 NR 024726
Thermosipho sp. FD1 AB10770
Thermosipho globiformans AB257289
Uncultured Thermosipho sp. clone NRB47 HM041964
Thermosipho ferriphilus AF491334
Thermosipho sp. Rift-s3 KF931642
Thermosipho atlanticus DV1140 NR 029020
Thermosipho sp. TH70-3 AB260053
Uncultured bacterium clone FS118-49B-02 AY869689
Uncultured bacterium clone ODP63B-02 AY704395
Thermosipho geolei strain DSM 13256 NR 025389
Uncultured Thermosipho sp. clone NRB46 HM041963
Uncultured bacterium clone PNG War B93 JF935229
to other Thermotogae
Thermosipho sp. 1070 CP007121
Thermosipho sp. MV1063 AJ419874
Thermosipho sp.1063 CP007223
Thermosipho sp. 1074 LBEX00000000
Thermosipho affectus ik275mar NR 117284
Thermosipho sp. 1223 LBEY00000000
Uncultured Thermotogales bacterium clone 609 AJ874306
Thermosipho sp. 2F70-1 EU418441
Thermosipho melanesiensis BI430 JYCX00000000
Thermosipho melanesiensis BI431 CP007389
Thermosipho melanesiensis BI432 JYCY00000000
Thermosipho melanesiensis BI433 JYCZ00000000
Thermosipho melanesiensis BI434 JYDA00000000
Thermosipho melanesiensis BI487 JYDB00000000
Thermosipho melanesiensis BI429 CP000716
0.05

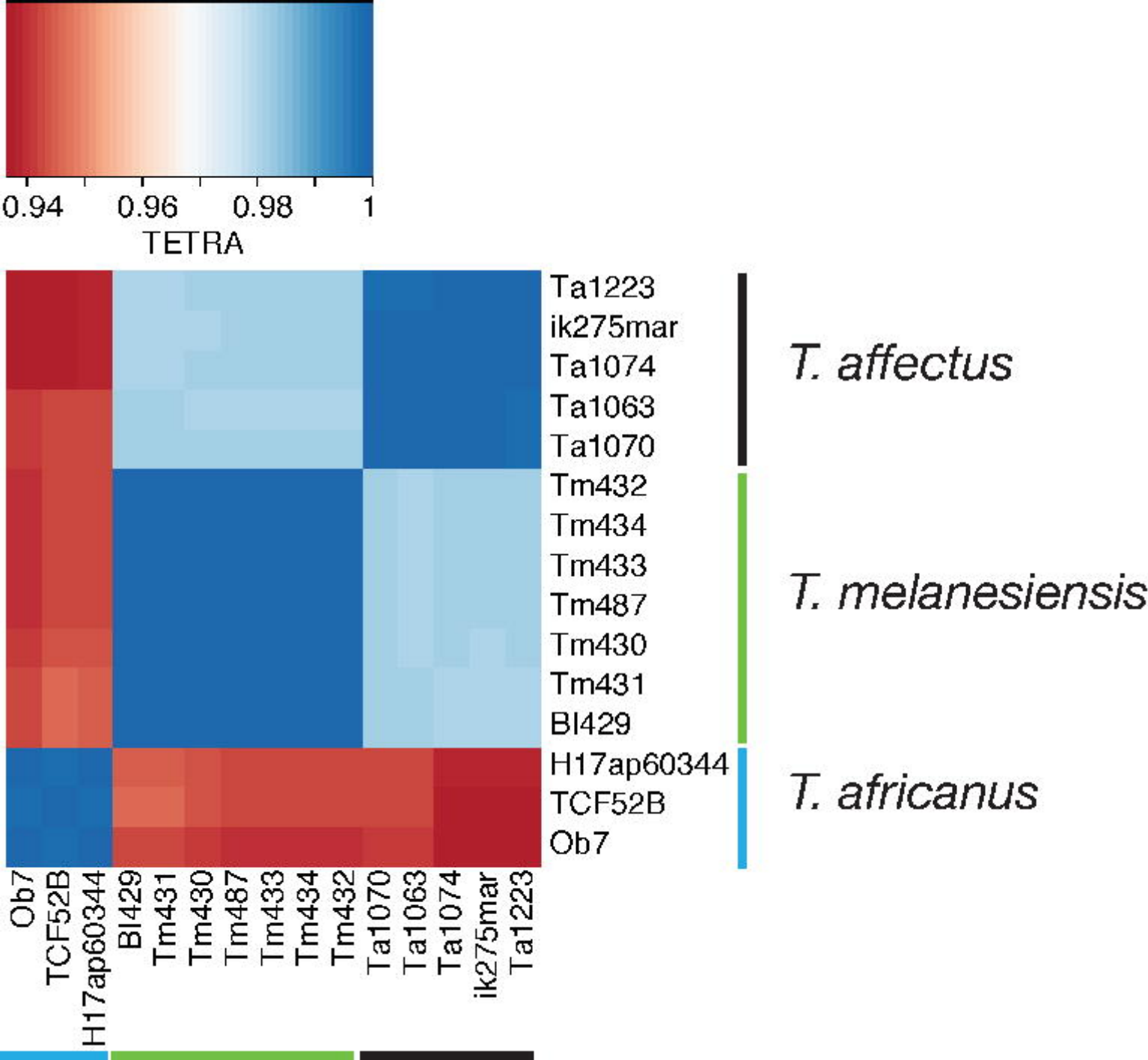
0.94
0.96
0.98
1
TETRA
Ta1223
ik275mar
Ta1074
Ta1063
Ta1070
Tm432
Tm434
Tm433
Tm487
Tm430
Tm431
Bl429
H17ap60344
TCF52B
Ob7
T. affectus
T. melanesiensis
T. africanus
Ob7
TCF52B
H17ap60344
Bl429
Tm431
Tm430
Tm487
Tm433
Tm434
Tm432
Ta1070
Ta1063
Ta1074
ik275mar
Ta1223

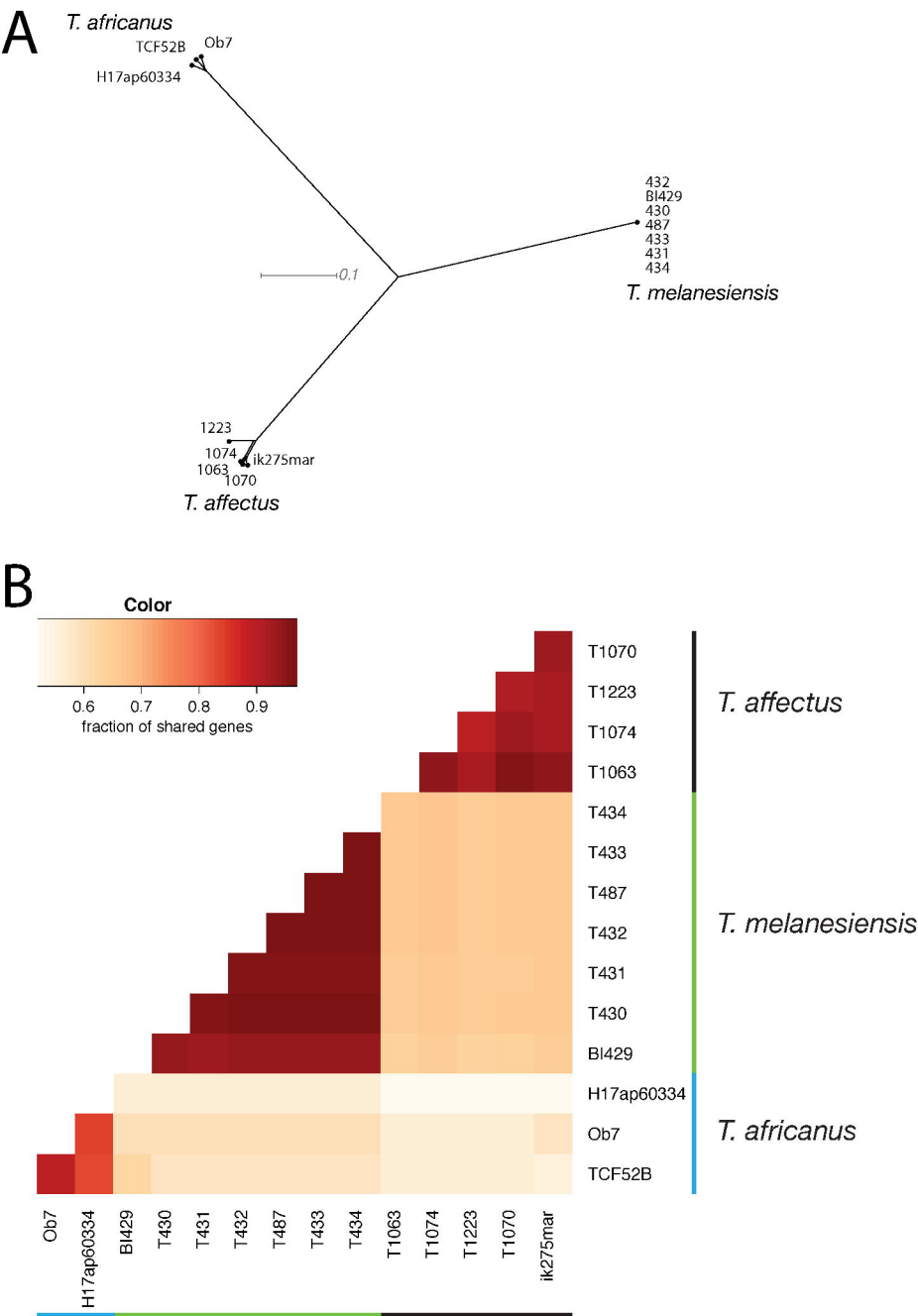
A
T. africanus
TCF52B
Ob7
H17ap60334
0.1
432
BI429
430
487
433
431
434
T. melanesiensis
1223
1074
1063
1070
ik275mar
T. affectus
B
Color
0.6
0.7
0.8
0.9
fraction of shared genes
T1070
T1223
T1074
T1063
T434
T433
T487
T432
T431
T430
BI429
H17ap60334
Ob7
TCF52B
T. affectus
T. melanesiensis
T. africanus
Ob7
H17ap60334
BI429
T430
T431
T432
T487
T433
T434
T1063
T1074
T1223
T1070
ik275mar

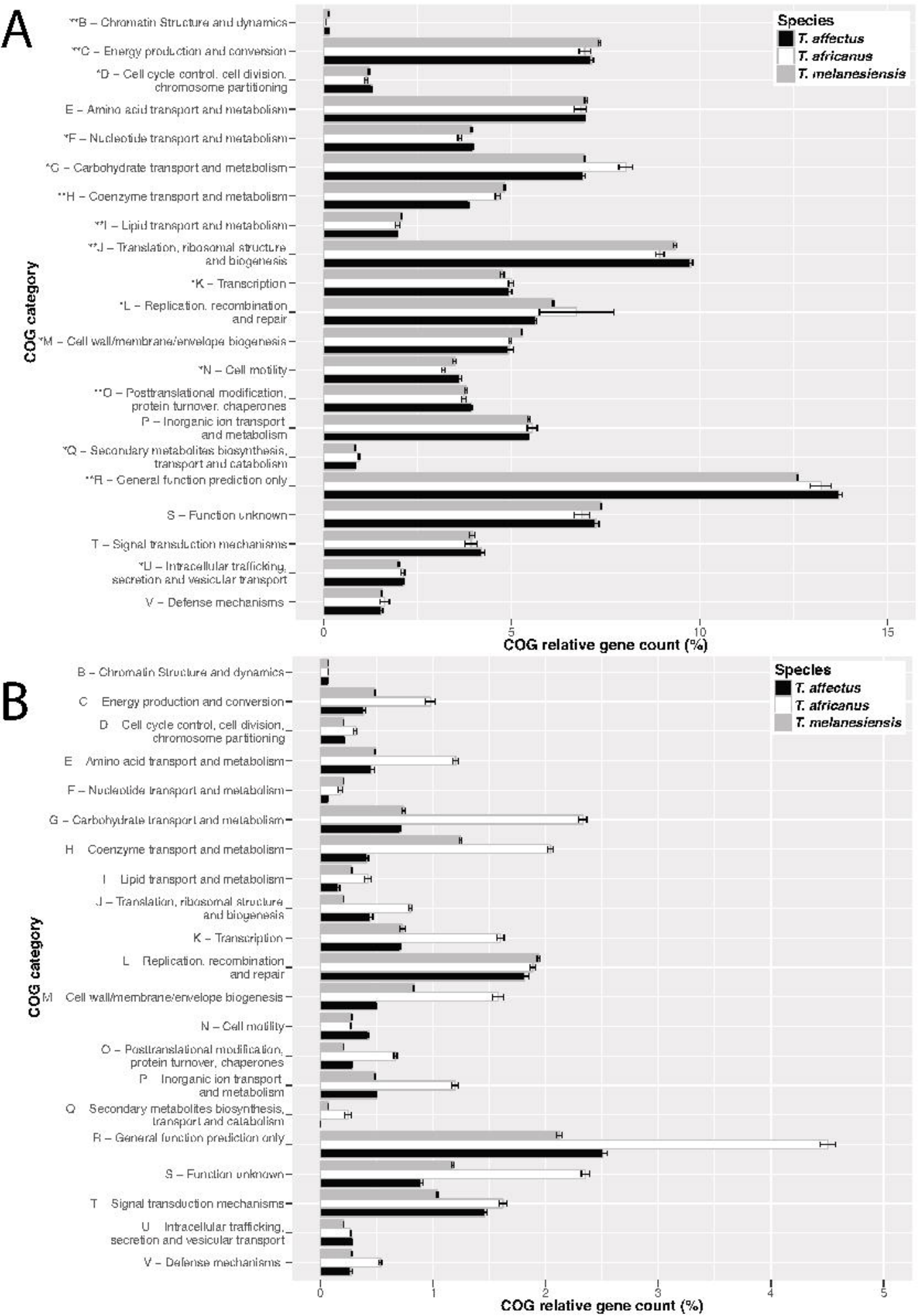
A
**B – Chromatin Structure and dynamics
**C – Energy production and conversion
*D – Cell cycle control, cell division, chromosome partitioning
E – Amino acid transport and metabolism
*F – Nucleotide transport and metabolism
*G – Carbohydrate transport and metabolism
**H – Coenzyme transport and metabolism
**I – Lipid transport and metabolism
**J – Translation, ribosomal structure and biogenesis
*K – Transcription
*L – Replication, recombination and repair
*M – Cell wall/membrane/envelope biogenesis
*N – Cell motility
**O – Posttranslational modification, protein turnover, chaperones
P – Inorganic ion transport and metabolism
*Q – Secondary metabolites biosynthesis, transport and catabolism
**R – General function prediction only
S – Function unknown
T – Signal transduction mechanisms
*U – Intracellular trafficking, secretion and vesicular transport
V – Defense mechanisms
COG category
Species
T. affectus
T. africanus
T. melanesiensis
0
5
10
15
COG relative gene count (%)
B
B – Chromatin Structure and dynamics
C Energy production and conversion
D Cell cycle control, cell division, chromosome partitioning
E Amino acid transport and metabolism
F – Nucleotide transport and metabolism
G – Carbohydrate transport and metabolism
H Coenzyme transport and metabolism
I Lipid transport and metabolism
J – Translation, ribosomal structure and biogenesis
K – Transcription
L Replication, recombination and repair
M Cell wall/membrane/envelope biogenesis
N – Cell motility
O – Posttranslational modification, protein turnover, chaperones
P Inorganic ion transport and metabolism
Q Secondary metabolites biosynthesis, transport and catabolism
R – General function prediction only
S – Function unknown
T Signal transduction mechanisms
U Intracellular trafficking, secretion and vesicular transport
V – Defense mechanisms
COG category
Species
T. affectus
T. africanus
T. melanesiensis
0
1
2
3
4
5
COG relative gene count (%)

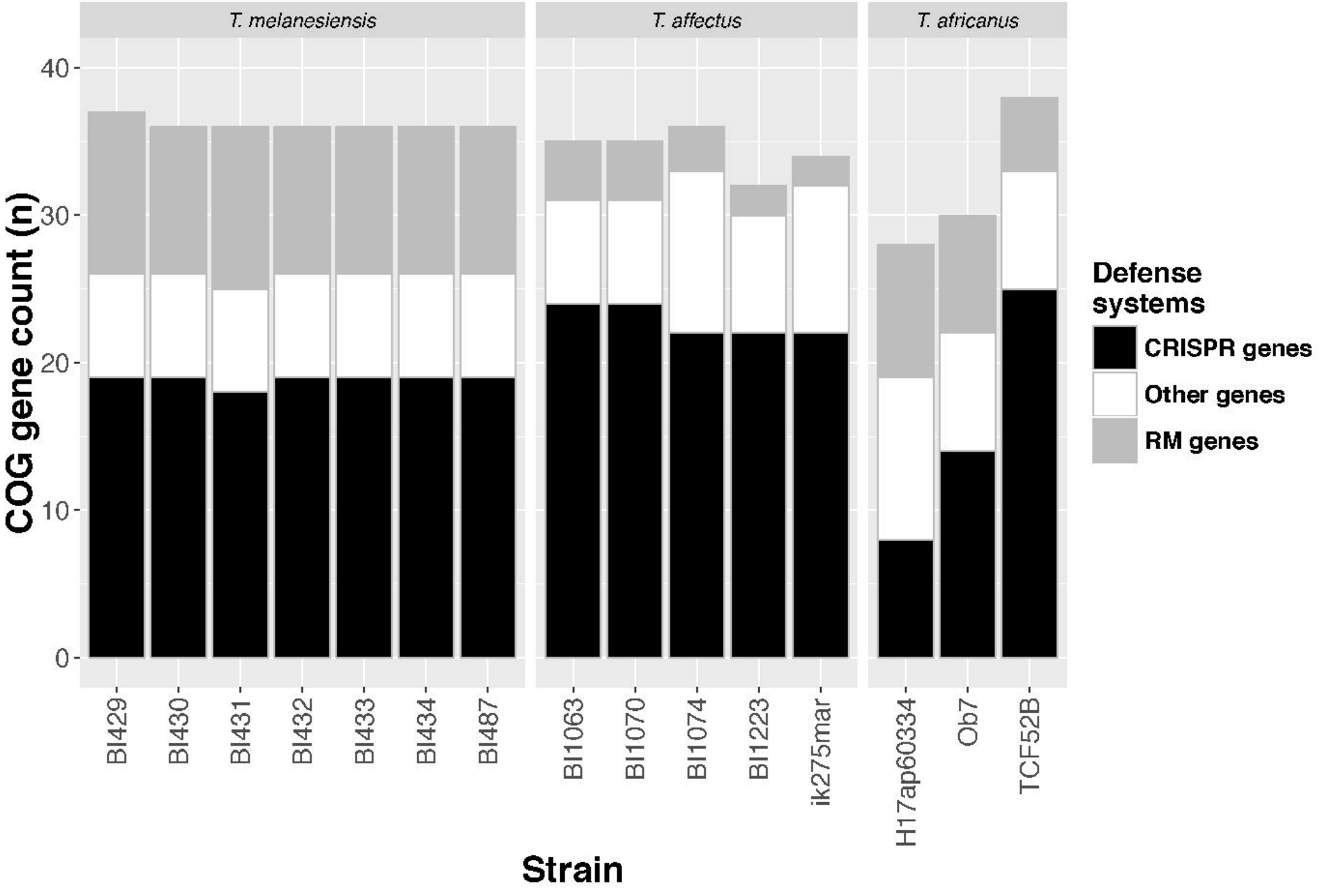
T. melanesiensis
T. affectus
T. africanus
COG gene count (n)
0
10
20
30
40
BI429
BI430
BI431
BI432
BI433
BI434
BI487
BI1063
BI1070
BI1074
BI1223
ik275mar
H17ap60334
Ob7
TCF52B
Strain
Defense systems
CRISPR genes
Other genes
RM genes